

Article

A New Webbing *Aberoptus* Species from South Africa Provides Insight in Silk Production in Gall Mites (Eriophyoidea)

Philipp E. Chetverikov ^{1,*}, Charnie Craemer ², Vladimir D. Gankevich ¹, Andrey E. Vishnyakov ¹
and Anna S. Zhuk ¹

¹ Department of Invertebrate Zoology, St. Petersburg State University, Universitetskaya Nab. 7/9, 199034 St. Petersburg, Russia

² Manaaki Whenua—Landcare Research, 231 Morrin Road, Auckland 1072, New Zealand

* Correspondence: philipp-chetverikov@yandex.ru

Abstract: Arthropods include a high diversity of lineages adapted for silk production. Several species of microscopic phytophagous mites of the hyperdiverse superfamily Eriophyoidea spin web; however, the origin of their silk is unknown. We described a new web-spinning mite, *Aberoptus schotiae* n. sp., collected from leaves of *Schotia brachypetala* (Fabaceae) in South Africa and showed that it has a complex life cycle, including two morphotypes of adults and nymphs. Molecular phylogenetic analyses and 28S sequence comparison showed conspecificity of heteromorphic females and rejected synonymy of *Aberoptus* and *Aceria* proposed by previous authors. For the first time, we provided SEM images of the web nests and, using a set of different microscopic techniques, described the silk-producing anal secretory apparatus (ASA) of *Aberoptus*. It comprises two pairs of anal glands (hypertrophied in web-spinning females), three cuticular sacs and a rectal tube leading to the anal opening. This is a unique case (analogy) of anal silk secretion in Chelicerata previously reported only in *Serianus* (Pseudoscorpiones). Recent findings of rudimentary ASA in distant eriophyoid lineages and the results of this study transform the current paradigm of exoticism of web-spinning eriophyoid taxa into the concept of synapomorphic specialization of the hindgut for excreting the anal gland secretions in Eriophyoidea.

Keywords: integrative taxonomy; anal gland; web-spinning; intestine; rectum; hindgut; Fabaceae; dimorphism



Citation: Chetverikov, P.E.; Craemer, C.; Gankevich, V.D.; Vishnyakov, A.E.; Zhuk, A.S. A New Webbing *Aberoptus* Species from South Africa Provides Insight in Silk Production in Gall Mites (Eriophyoidea). *Diversity* **2023**, *15*, 151. <https://doi.org/10.3390/d15020151>

Academic Editor: Luc Legal

Received: 26 December 2022

Revised: 12 January 2023

Accepted: 17 January 2023

Published: 21 January 2023



Copyright: © 2023 by the authors. Licensee MDPI, Basel, Switzerland. This article is an open access article distributed under the terms and conditions of the Creative Commons Attribution (CC BY) license (<https://creativecommons.org/licenses/by/4.0/>).

1. Introduction

Silks are secreted fibrous materials consisting of protein threads composed of repeating arrays of polypeptides [1]. Members of various terrestrial and aquatic arthropod lineages deposit or spin silks, and silks play a crucial role in their survival and reproduction [2]. In the forms of various cocoons, webs, nests, or solitary threads, silk serves to provide shelter and structural support and aid in reproduction, dispersal, and foraging or capturing [3]. Silk obtained from the cocoons of the mulberry silkworm *Bombyx mori* (Lepidoptera) reared in captivity is a long-known natural source of high-quality textile widely used by humans, especially in Asia, since the end of the Neolithic period [4]. Nowadays, the silk fibers from *B. mori* are used in clothing, furniture, biomedicine, and the industry, and attempts to benefit from silks of spiders and other less common silk producers are regularly taken [5–10].

Silk production is known in three euarthropod clades: Myriapoda (in Diplopoda, Symphyla, and Chilopoda), Hexapoda (in seventeen orders), and Arachnida (in all Aranei, Pseudoscorpiones, and some Acari) [1,11]. Different glands associated with the stomodeum, Malpighian tubules, and a variety of dermal glands have evolved in these clades to produce silks [1,12,13]. Silk glands associated with the stomodeum are the most common. This group includes prosomal (podocephalic, infracapitular, and palpal) glands known or suspected in various superfamilies of acariform mites (Cheyletoidea, Bdelloidea, Raphignathoidea,

Eupodoidea, Tydeoidea) and all pseudoscorpiones, and labial glands of insects [1,14]. The latter is present in larvae of butterflies, moths, caddisflies, fleas, and various hymenopterans and dipterans; in adult females of booklice (Psocoptera) and some wasps (Hymenoptera: Vespidae); and in all stages of crickets (Orthoptera: Gryllacrididae and Anostostomatidae) [2].

Silk-producing dermal glands are less numerous in insects and mites; however, all known silk glands in myriapods fall into this category [11]. In insects, dermal glands are situated on prothoracic tarsomeres in all stages of webspinners (Embiidina), males of some dagger flies (Diptera: Empididae), and on the abdomen or posterior metasoma in some wasp females, or are associated with the reproductive system, e.g., accessory genital glands in males of some primitive insects (Archaeognatha and Zygentona) and colleterial glands in females of water beetles (Hydrophilidae) and lacewings (Neuroptera) [2]. The only case of specialized silk produced by dermal glands in arachnids is reported in water mites (Hydrachnidia) [15].

Malpighian tubule silks are the least common in arthropods. They are known only in larval insects: in lacewings and ant lions (Neuroptera), thrips (Thysanoptera), mayflies (Ephemeroptera: Polymitarcyidae), and plant-eating beetles (Coleoptera: Cucujiformia) [2]. In this case, the silk is secreted into the hindgut and excreted through the anus [16]. A similar way for excreting the silk through the anal opening is known in males of a single pseudoscorpion taxon (*Serianus* sp.) possessing an endodermal rectal pocket secreting silk for marking a path to the spermatophore with silken threads [17]. Finally, several gall mites of the superfamily Eriophyoidea possess anal glands associated with the rectum that were also hypothesized to produce a silk-like substance excreted through the anus [18,19].

Among Acari, silk production or the ability to spin is documented for a number of acariform mites of the suborder Prostigmata (Acariformes: Trombidiformes), whereas no examples of silk production in parasitiform and sarcoptiform mites are known [14,20,21]. In prostigmatans, silk production may function to protect habitats, eggs, or spermatophores, to produce signal and securing threads, transport threads, or webs used for ballooning, and to establish molting nests, capture nets, and threads [14,22]. Protecting the eggs from predation and regulating the relative humidity around the eggs are important functions of silks in various mites, including economically important herbivore groups, such as spider mites [22,23].

Eriophyoidea is one of the silk-producing groups of phytophagous acariform mites. It was traditionally assigned to Prostigmata [24], but recent morphological and molecular phylogenetic studies inferred Eriophyoidea as a basal acariform lineage sister to soil-inhabiting nematalycid mites outside Trombidiformes [25–27]. Eriophyoids are morphologically simplified microscopic mites with an elongated body, two pairs of legs, and needle-like stylets which they use for piercing plant cells and sucking the cell sap [28]. Due to their ability to vector viruses, induce gallogenesis, and affect the photosynthetic efficiency and primary metabolite production in plant tissues, many species of Eriophyoidea are economically important pests of crops [29–31]. Members of the four eriophyoid genera, *Aberoptus*, *Aceria*, *Cisaberoptus*, and *Aculops* have been found living under silk-like webbing (Figure 1) which they produce on their host plants, usually along leaf veins and on petioles [32,33]. Serological tests of the webbing produced by *Aculops knorri* Keifer 1976 on leaves of *Lepisanthes rubiginosa* (Roxb.) Leenh. (Sapindaceae) collected at two localities in Thailand proved the web to be true proteinaceous silk [34].



Figure 1. Microphotographs of the web nests of three eriophyid species from South Africa. (A–C)—young (A,B) and older (C) nests of *Cisaberoptus kenyae* on mango leaves; (D)—webbing of *Aberoptus platessoides* (arrows) on petioles of leaves of *Ochna pretoriensis*; (E)—a female of *A. platessoides* (arrow) in the nest, web partially removed; (F)—webbing of *Aberoptus schotiae* n. sp. on lower leaf surface of *Schotia brachypetala*; (G)—a group of web-spinning females of *A. schotiae* n. sp. (arrowheads) under web. Scale bars: (A–D,F) = 0.5 cm; (E,G) = 100 μ m.

Web producers of the genera *Aberoptus* Keifer and *Cisaberoptus* Keifer possess several unique modifications of the gnathosoma or legs that could be attributed to their web-spinning ability and indicate that the mites “... remain fixed for considerable periods of time” [35]. *Cisaberoptus kenyae* Keifer 1966, the type species of the genus *Cisaberoptus*, possesses a spatulate terminal segment of each palp forming a sucker-like structure and legs I and II with large pad-like equally shaped empodia with a high number of empodial rays (16–18), shortened tarsi, and tibiae, and partially fused genu and femur. This species is widespread in southern and south-eastern Asia, Africa, and South America. It lives under

a fine web coating on mango leaves (*Mangifera indica* L., Anacardiaceae) (Figure 1A–C) [36] and causes yellowing and premature dropping of leaves [30,36].

Genus *Aberoptus* has seven species associated with arborous plants of the families Fabaceae, Ochnaceae, and Anacardiaceae and is described from South Africa, Brazil, Taiwan, and Samoa. *Aberoptus* spp. have a typical eriophyoid-structured gnathosoma but greatly modified legs with heteromorphic empodia I and II, a spatulate structure on tarsus I, and two shortened terminal leg segments [28].

Several studies have described morphological dimorphism in populations of web-spinning eriophyoids. In *C. kenyae* and in two *Aberoptus* spp., heteromorphic females, called deutogynes and protogynes, were found under the web [36–38]. The deutogyne females possess the specialized morphological structures mentioned above, spin the web nests, reproduce, and migrate to form new nests. The protogynes survive only under the web and have the typical morphology of the genera *Aceria* or *Aculops*, devoid of modified legs and gnathosoma [33]. Males of the Brazilian species *Aberoptus inusitatus* are also dimorphic and morphologically resemble their corresponding forms of females [33]. The presence of *Aceria*- or *Aculops*-like mites was reported in populations of *A. samoae* and *A. platessoides* [35,39]. Finally, a new *Aceria* was recently described from under the web of *C. kenyae* from Egypt [40], which is morphologically very similar to the protogynes of *C. kenyae* reported from Brazil [37]. According to the assumption that generic diagnoses should be based on the morphology of protogynes, *Aceria* was proposed a senior synonym of *Aberoptus* [33], although some authors disagreed with this concept and called for future efforts to resolve this taxonomic uncertainty [19,28,36].

The web-spinning mechanism of eriophyoids is poorly understood and has not yet been studied. However, in slide-mounted deutogynes of two Brazilian *Aberoptus* spp., a complex of unusual cuticular structures was discovered. It comprises “... a pair of branched tubules, two saccular elongate structures fused to a median globular reservoir that opens to the exterior through a pair of parallel ducts, each ending in a caudal lobe” [33,38]. Later, similar but less developed cuticular structures were observed in various genera (*Phyllocoptes*, *Setoptus*, *Loboquintus*, *Pentasetacus*, *Rhyncaphytoptus*) representing all major phylogenetic lineages of Eriophyoidea [41–43]. In *Phyllocoptes bilobospinosus* Chetverikov 2019, the remnants of putative large anal glands and their cuticular ducts connected with a rectal sac that continued with the rectal tube ending with an anal opening, were observed in the caudal body region of partially cleared specimens. This complex of internal structures associated with the rectum was termed the “anal secretory apparatus” (ASA), considered a synapomorphy of Eriophyoidea, and presumed to function for silk production in gall mites [19].

In the early 2000s, the outstanding South African scientist and naturalist Dr. S. Naser (16.IV.1942–17.II.2021) informed us about his discovery of eriophyoids living under white web-coating on leaves of *Schotia brachypetala* (Figure 1E,G) in South Africa. Since then, we have collected these mites from the same tree near a church in the center of Pretoria many times. Our microscopic investigations showed that (a) they belong to a new species and (b) two morphotypes are present in the model population—*Aberoptus*-like and *Aceria*-like. In this paper, we aim to describe the new species, test the conspecificity of the two morphotypes, investigate the organization of the ASA and the web nests using a wide range of techniques, and assess the phylogenetic positions of *Aberoptus* and *Cisaberoptus* and their relationships with *Aceria*.

2. Materials and Methods

Collection and morphological measurements. The leaves of the same model tree of *Schotia brachypetala* Sond. (Fabaceae) with white spots of the mite webbing on the lower and upper surfaces were sampled in Pretoria (South Africa) in February 2003, March 2013, April 2015, and November 2013, 2016, and 2017. The leaves were examined under a stereo microscope, and the mites were collected from under the web using a minuten pin. Some mites were slide-mounted in a modified Berlese medium with Iodine [44] and cleared

on a heating block at 90 °C for 3–5 h. The rest of the mites were stored in Eppendorf tubes filled with 96% ethanol or kept alive on leaves in a refrigerator (+4 °C) for further examination. Among 410 slide-mounted specimens of *Aberoptus n. sp.*, 280 were collected in November and 130 in March and April. For estimation of the seasonal abundance of different morphotypes in the samples, all mites collected in spring or autumn were treated as two seasonal data arrays, and the percentage values were calculated for females, males, nymphs, and larvae collected in different seasons.

External morphology of the slide-mounted specimens was studied using conventional light microscopy (LM) using a Leica DM2500 and photographed with a TouPCam UC-MOS09000KPB digital camera. Morphological descriptions were based on phase contrast (PC) and differential interference contrast (DIC) LM observations and supplemented with LT-SEM data (see below). All measurements were obtained using the TouPCam TouPCView software. They were given in the descriptions in micrometers (μm) and were lengths except when stated otherwise. The measurements of the web-spinning females were based on the holotype, whereas the ranges (in brackets) were based on measurements of the paratypes and holotype. In the descriptions of all other instars, only ranges were given. Terminology of eriophyoid morphology and classification of Eriophyoidea follow [24] and [28], respectively. Drawings of mites were sketched by pencil using a video projector [45] and were scanned and finalized in Adobe Illustrator CC 2014 using a Wacom Intuos S (CTL-4100K-N) graphics tablet.

Low-temperature scanning electron microscopy (LT-SEM). For LT-SEM, fragments of the infested *Schotia* leaves and live mite specimens collected in February 2003 were placed on a double-sided carbon tape with the aid of a minute pin tool under a stereomicroscope. The piece of tape with the mites was pasted onto a sample holder, and the modified version of the cryo-fixation technique (from [46]) was used for preparing the samples. The sample holder with mite material was plunged frozen in liquid nitrogen slush and transferred to a conventional JEOL JSM 840 SEM with a cryo-stage pre-cooled to about -170 °C. The samples were thereafter etched for about 30 min at -80 °C and sputter-coated with gold. The samples were then observed at an accelerating voltage of 5 kV or 2 kV (to prolong viewing time and alleviate charging).

Atomic Force Microscopy (AFM). The fragments of *Schotia brachypetala* about 0.5 cm \times 0.5 cm with mature web nests collected in April 2015 were observed using Probe nanolaboratory INTEGRA-AURA equipped with NSG10 cantilevers (NT-MDT SI, Moscow, Russia) that were applied for scanning and measurements in a non-contact mode of AFM.

Confocal laser scanning microscopy (CLSM). CLSM was used for investigating the topography of the internal cuticle-lined elements of the anal secretory apparatus (ASA) of the mites. For this purpose, 23 web-spinning females collected in November 2016 and kept in vials with 96% ethanol were rinsed in 70% ethanol for 2 h, and, after that, rinsed again in hot (+70 °C) distilled water for 3 h to make exoskeletons softer after dehydration in 96% ethanol. Thereafter, the mites were mounted in Hoyer's medium ([44], p. 387), which is the medium of choice for capturing autofluorescence of the eriophyoid mite cuticle under CLSM [47]. CLSM acquisition was carried out using a Spectral confocal and multiphoton system Leica TCS SP2 with objectives 40 \times N.A. 1.25–0.75 Oil CS HCX PL APO and 63 \times N.A. 1.4–0.60 Oil IBL HCX PL APO using previously described adjustments [48]. Image stacks were merged into maximum intensity projections (MIP) with the aid of the reconstruction software ImageJ [49]. A series of images with a gradually increasing depth of focus of one female (with almost intact ASA of the best quality) was used to illustrate the elements of ASA in the new species.

Transmission electron microscopy (TEM). For anatomical observations, live mites collected in November 2016 were fixed in 2.5% glutaraldehyde (buffered in 0.1 M Na-cacodylate, pH 7.4) for four hours at +4 °C, washed with the same buffer, treated with 1% tetroxide osmium for 1 h, washed twice in distilled water, dehydrated in increasing ethanol series (30, 50, 70, 96, 100%), and embedded in SPURR resin (Sigma EM0300-1KT). Thin sections of eight web-spinning females were prepared using a Leica EM UC7

ultramicrotome, immersed in a saturated solution of uranyl acetate for 20 min and lead citrate for 5 min, and photographed using an electron microscope Jeol JEM-1400 with a digital CCD camera.

Light microscopy of serial semi-thin sections (LMSSS). Serial semi-thin transverse and longitudinal sections of the mites from the blocks embedded for transmission electron microscopy were stained according to [50] and examined and photographed with a Leica DM2500 light microscope coupled with a Leica Flexacam C1 (Leica Microsystems GmbH Wetzlar, Germany) digital camera.

DNA extraction and sequencing. For DNA extraction, 4 large females of morphotype A (with distinctly elongated telosome) and 3 smaller females of morphotype B (with clearly blunt caudal lobe) were crushed separately with a fine pin in a 2 μ L drop of distilled water on a cavity well microscope slide. The fragments of the anterior part of the mite bodies (including morphotype-specific legs) were pulled out of the drop and slide-mounted for morphotype confirmation. Each drop was pipetted into a thin-walled PCR tube with 20 μ L of 12% solution of Chelex[®] 100 Resin Bio Rad before being heated three times (5 min at 95 °C) in a thermostat with intermediate short vortexing. The solution above the Chelex[®] granules was used as the DNA template for PCR to amplify the *D1–D2* domains of the 28S rDNA. For the PCR and sequencing, we applied the protocols and primers detailed by [43]. Sequences were obtained using BigDye Terminator v.3.1 chemistry (Applied Biosystems, Foster City, CA, USA) and a 3500xl Genetic Analyzer (Applied Biosystems).

Sequence alignment and molecular phylogenetic analyses. Molecular phylogenetic analyses of *D1–D2* 28S sequences of eriophyoid mites were done to assess the phylogenetic positions of the web-spinning genera *Aberoptus* and *Cisaberoptus* and their relationships with members of the genus *Aceria*. For this purpose, on the web site of GenBank, we blasted the sequences of *D1–D2* 28S of *Aberoptus schotiae* n. sp. against Eriophyidae and filtered the sequences by coverage 40–100%. We then removed all identical sequences of the same species. The resultant FASTA file included numerous sequences of *Aceria* spp. from monocot and eudicot hosts, one sequence of *Cisaberoptus* (KT070272), and two sequences of *Aberoptus* (KT070266 and OP419490). Sequences of *Nanorchestes* (KY921973) and four sequences of Phytoptidae (KY921988–KY921991) were used respectively as distant and close out-groups in our analyses. We combined them with the previously mentioned sequences of Eriophyidae and obtained the final dataset of 290 sequences. These sequences were aligned with the MAFFT algorithm [51] through the web-based program interface [52] using default settings and the 28S alignment from [26] as a reference.

Aligned 28S sequences were trimmed from the 3' and 5' ends. The final alignment contained 290 sequences with 1447 nucleotide positions representing *D1–D2* regions of the 28S gene. Maximum likelihood analyses were conducted in IQ-tree 2 [53]. For gene evolution, the TIM2+F+R9 model was selected using ModelFinder [54] as implemented in IQ-tree 2 based on the Bayesian Information Criterion. Branch support values were generated from Ultrafast bootstrap approximation (UFBoot) with 10,000 bootstrap alignments, 1000 maximum iterations, and a minimum correlation coefficient of 0.99. Values of a single branch test (SH-like approximate likelihood ratio test (SH-aLRT)) with 1000 replicates were labeled on the maximum likelihood (ML) trees.

3. Results

3.1. Taxonomy: Morphological Description of *Aberoptus Schotiae* n. sp.

Genus *Aberoptus* Keifer, 1951

Diagnosis. Members of this genus have an adult female morphotype adapted for web-spinning. The generic diagnosis was based on this morphotype. The web-spinning form of the female has uncommonly shaped legs: tibia I with distal rounded spatulate projection, empodia I and II heteromorphic, and fused or indistinctly separated genu, and femur of both legs forming together a consolidated segment. Empodium I of typical structure (except bristle-shaped in *A. samoae* Keifer, 1951). Empodium II widened, pad-like with many lateral rays and additional rows of rays on the ventral surface of the empodium. Opisthosoma

dorsoventrally flattened with subequal dorsal and ventral annuli. Ventral opisthosomal annuli behind external genitalia with faint, reduced, or sparser microtubercles resulting in a “bald spot” of the smoother cuticle. Scapular setae *sc* on the posterior shield margin, directed divergently posteriorly. All usual opisthosomal setae present, except *h1* absent in some species. Very short setae *h2*. Caudal lobe elongated and tapered. Well-developed anal secretory apparatus (ASA) present, typically observed in slide-mounted specimens as two paired cuticular tubes associated with the rectum. Non-spinning form of females is known in three species and hypothesized in all members of the genus. It is of typical morphology of *Aceria* or *Aculops*, with a well-developed, widened, blunt bilobed caudal lobe, rudimentary ASA, and long setae *h2* (>40 µm).

Remarks. The origin of the spatulate projection is uncertain. According to [24], it is a derivate of tarsus I. However, if this spatula belongs to tarsus I, they together would function as an entire structure. Some of our LTSEM images (Figures S3 and S6), as well as Figure 1.1.1.21d in [24], suggested that the spatulate projection covers the tibiotarsal articulation I dorsomedially and may belong to tibia I. In this case, the mite could use the spatula for resting against the surface, and tarsus I can be independently used for accommodating the substrate irregularities. In this paper, contrary to the common interpretation of this structure as a derivate of tarsus I, we considered it to be of tibial origin.

Type species: *Aberoptus samoae* Keifer, 1951: 97, Figure 207

Species included. *Aberoptus cerostructor* Flechtmann, 2001 from *Hymenaea courbaril* L. (Fabaceae, Detarioideae) from Brazil; *A. championus* Huang, 2005 from *Bauhinia championii* Benth. (Fabaceae, Cercidoideae) from Taiwan; *A. integritas* Huang and Cheng, 2005 from *Sindora cochinchinensis* Benth. (Fabaceae, Cercidoideae) from Taiwan; *A. inusitata* Britto and Navia, 2008 in Britto et al. [33] from *Caesalpinia echinata* Lam. (Fabaceae, Caesalpinioideae) from Brazil; *A. platessoides* Smith Meyer, 1989 from *Ochna pretoriensis* E. Phillips (Ochnaceae) from South Africa; *A. samoae* Keifer, 1951 from *Mangifera indica* L. (Anacardiaceae) from Samoa; and *A. schotiae* n. sp. from *Schotia brachypetala* Sond. (Fabaceae, Detarioideae) from South Africa.

Remarks. *Cisaberoptus pretoriensis* Smith Meyer 1989 was described from South Africa “... occurring in association with *Aberoptus platessoides* and an *Aculops* sp. under a waxy layer on twigs, petioles and leaf-bases” of *Ochna pretoriensis* (Ochnaceae) [39]. According to the textual description and drawings, this species looks like a member of the genus *Aculops*. It lacks the spatulate terminal palp segments characteristic of genus *Cisaberoptus*, has “... leg segments normal and with all normal setae ...”, equally shaped typically structured seven-rayed empodia I and II, and faint “spot” of smoother cuticle between tubercles of opisthosomal setae *d*, typical of most *Aberoptus* species. *Aculops*-like morphology, the “spot”, and sympatry with *A. platessoides* indicate that *A. pretoriensis* may be a non-spinning form of *A. platessoides*. If confirmed, *A. pretoriensis* should be treated as a junior synonym of *A. platessoides*. Alternatively, although less probably, *C. pretoriensis* could belong to a new genus based on the unusual “strong rostrum with triangular projections anteriorly” [39] that may be an autapomorphy of *C. pretoriensis*.

Hosts and relation to host. Five of the seven known *Aberoptus* spp. are associated with Fabaceae (Fabales), one species with Ochnaceae (Malpighiales), and one species with Anacardiaceae (Sapindales). The ability to produce and spin silk seems to be characteristic of all known *Aberoptus* spp.; in particular, five species were found underneath webbing on leaves and/or petioles where they feed and reproduce (Figure 1). In the period when they leave the old nests and migrate to infest new vegetation and produce new nests, they can be found as vagrants.

Remarks. Although mango was indicated as the type host plant in the original description of *A. samoae*, [36] reported that “... the precise identification of the Samoan host of *samoae* is unknown ...” and therefore, it needs verification.

Distribution: Up to now *Aberoptus* spp. are known in four countries—Taiwan, South Africa, Brazil, and Samoa (Figure 2).

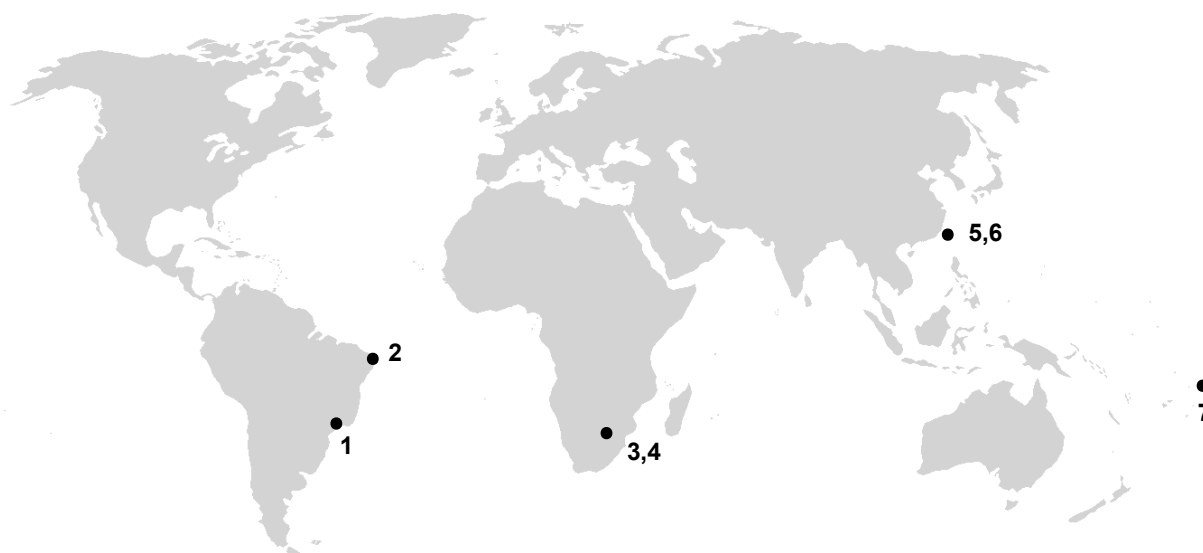
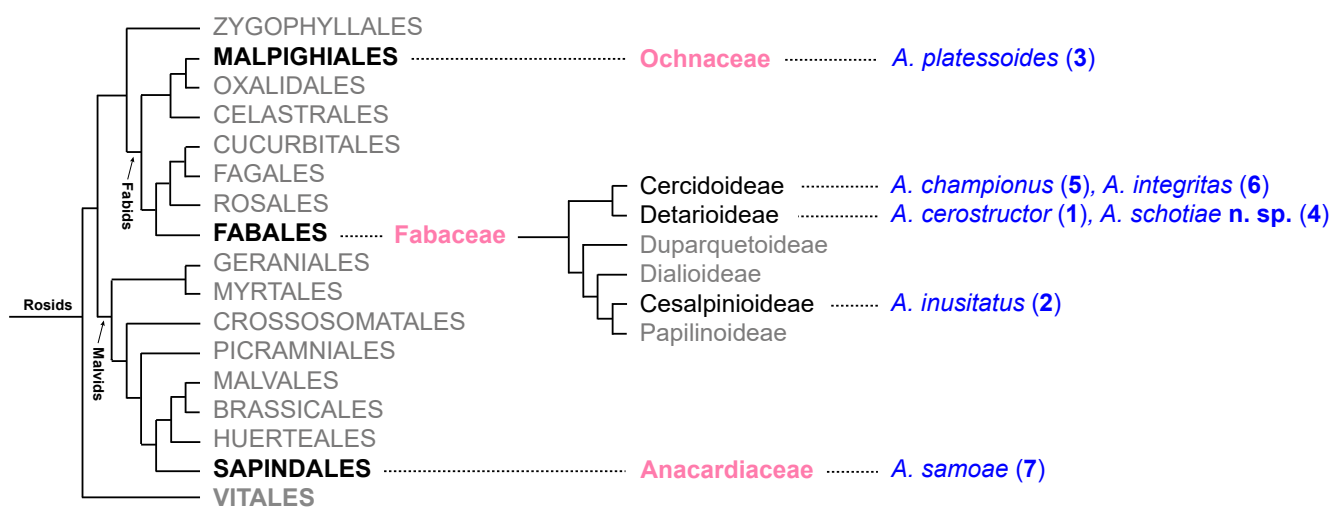


Figure 2. Distribution of *Aberoptus* spp. (blue) on the plant phylogeny (above) and findings of *Aberoptus* spp. in the world (below). The plant phylogeny follows [55]. Three host plant families are marked pink; phylogenetic relations between fabacean subfamilies follows [56]. Numbers in the map correspond to *Aberoptus* spp. indicated in the upper part of the figure.

Aberoptus schotiae n. sp.—Figures 3–7 and S1–S8.

Two morphotypes (A & B) of females, males, and nymphs, and one morphotype of larvae are present in our samples collected in different seasons. In this section, we described all observed morphotypes of adults and immatures of *Aberoptus schotiae* n. sp. The data on their seasonal distribution in our material are provided in Section 3.2.

FEMALE, morphotype A ($n = 10$). Body vermiform, notably narrowed caudally, slightly yellowish or reddish, 274 (256–289), 82 (74–87) wide at the level of setae c_2 . **Prodorsal shield** subrhomboid or subcordate, 36 (32–38), 75 (72–85) wide, with short subtriangular frontal lobe 5 (4–8), 8 (6–8) wide. Prodorsal shield and epicoxal areas smooth. Irregular longitudinal cuticular folds (appearing as lines) present in the medial part of the prodorsal shield in some slightly distorted slide-mounted specimens. Tubercles of setae sc situated in a notch behind the posterior shield margin, sc 33 (29–37), 44 (42–45) apart, directed divergently posteriorly.

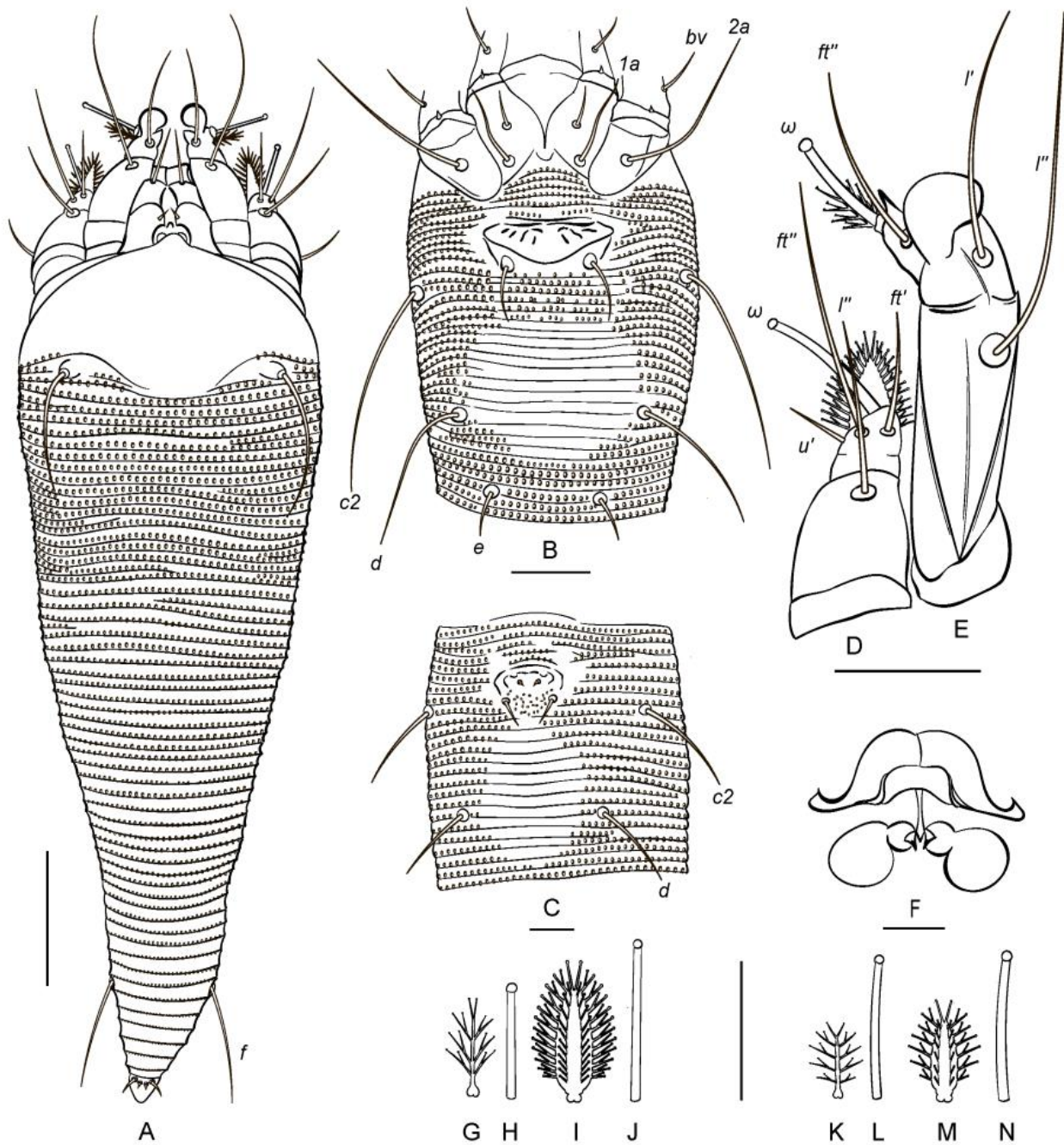


Figure 3. Drawings of female (A,B,D–J) and male (C,K–N) of *Aberoptus schotiae* n. sp. (morphotype A). (A)—dorsal view of entire female; (B)—female coxigenital area, note ventral ‘bald’ patch between setae *d*; (C)—male genital area; (D,E)—legs I and II; (F)—female internal genitalia; (G)—female empodium I, (H)—female tarsal solenidion I, (I)—female empodium II, (J)—female tarsal solenidion II; (K)—male empodium I, (L)—male tarsal solenidion I, (M)—male empodium II, (N)—male tarsal solenidion II. Scale bar: (A) = 30 μm; (B) = 15 μm; (C–E,G–N) = 10 μm; (F) = 5 μm.

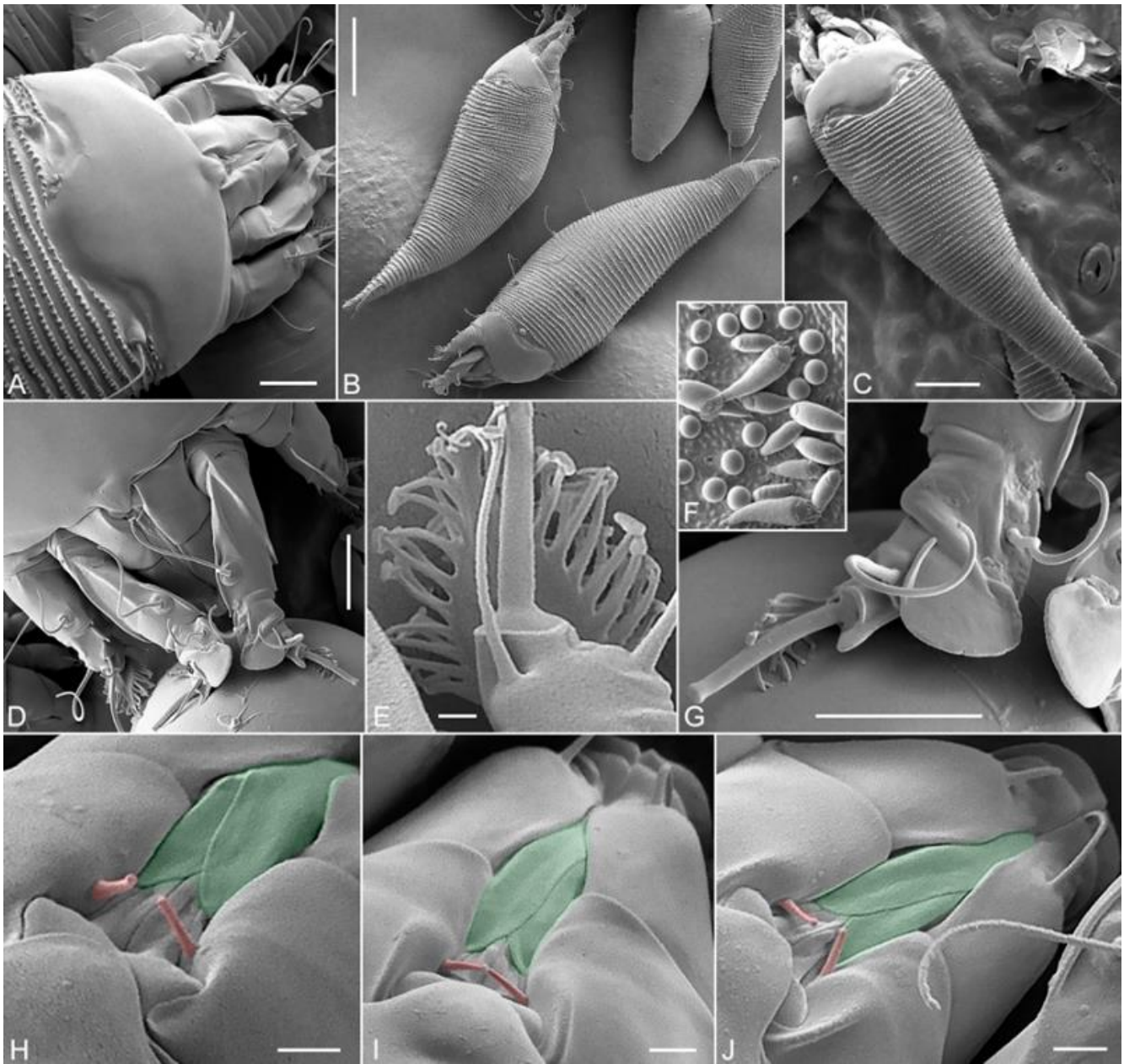


Figure 4. LTSEM images of morphotype A females (and partly shown immatures in backgrounds in A,B and in colony in F) of *Aberoptus schotiae* n. sp. (A)—dorsal view of anterior part of female; (B)—entire lateral (upper) and semi-lateral (bottom) mites; (C)—dorsal view of entire mite; (D)—dorsal view of gnathosoma and legs; (E)—dorsal view of apical part of tarsus II; (F)—colony underneath removed web nest; (G)—dorsal view of tibia and tarsus of leg I; (H–J)—dorsal view of gnathosoma in three females, stylet sheath and palpcoxal setae *ep* are colored green and red respectively. Scale bars: (A,D,G) = 10 μm ; (B) = 50 μm ; (C) = 30 μm ; (F) = 100 μm ; (E) = 1 μm ; (H–J) = 2 μm .

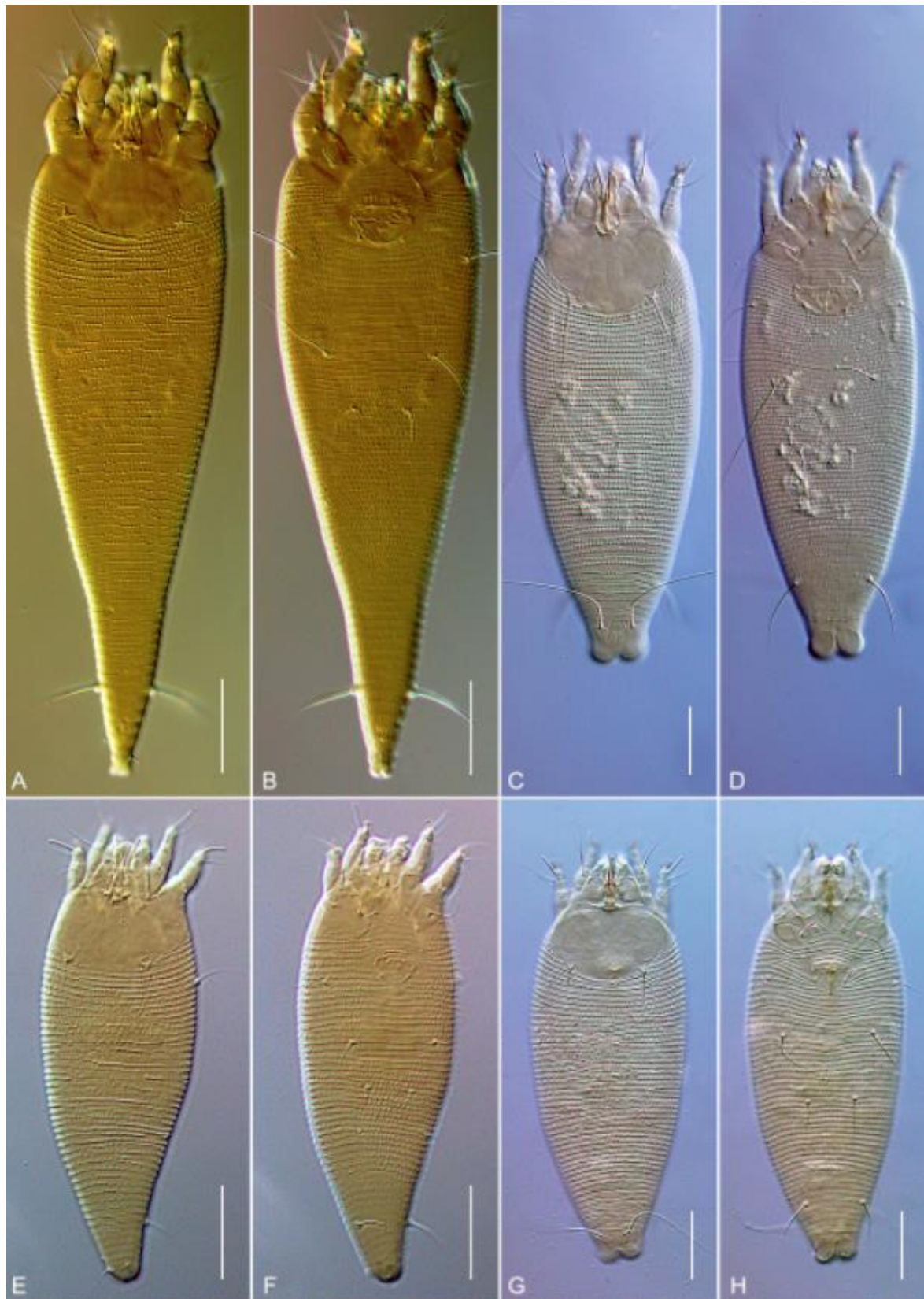


Figure 5. DIC LM images of females (A–D) and males (E–H) of morphotype A (A,B,E,F) and morphotype B (C,D,G,H) of *Aberoptus schotiae* n. sp. (A,C,E,G)—dorsal view; (B,D,F,H)—ventral view. Scale bars: (A,B,E,F) = 40 μ m; (C,D,G,H) = 30 μ m.

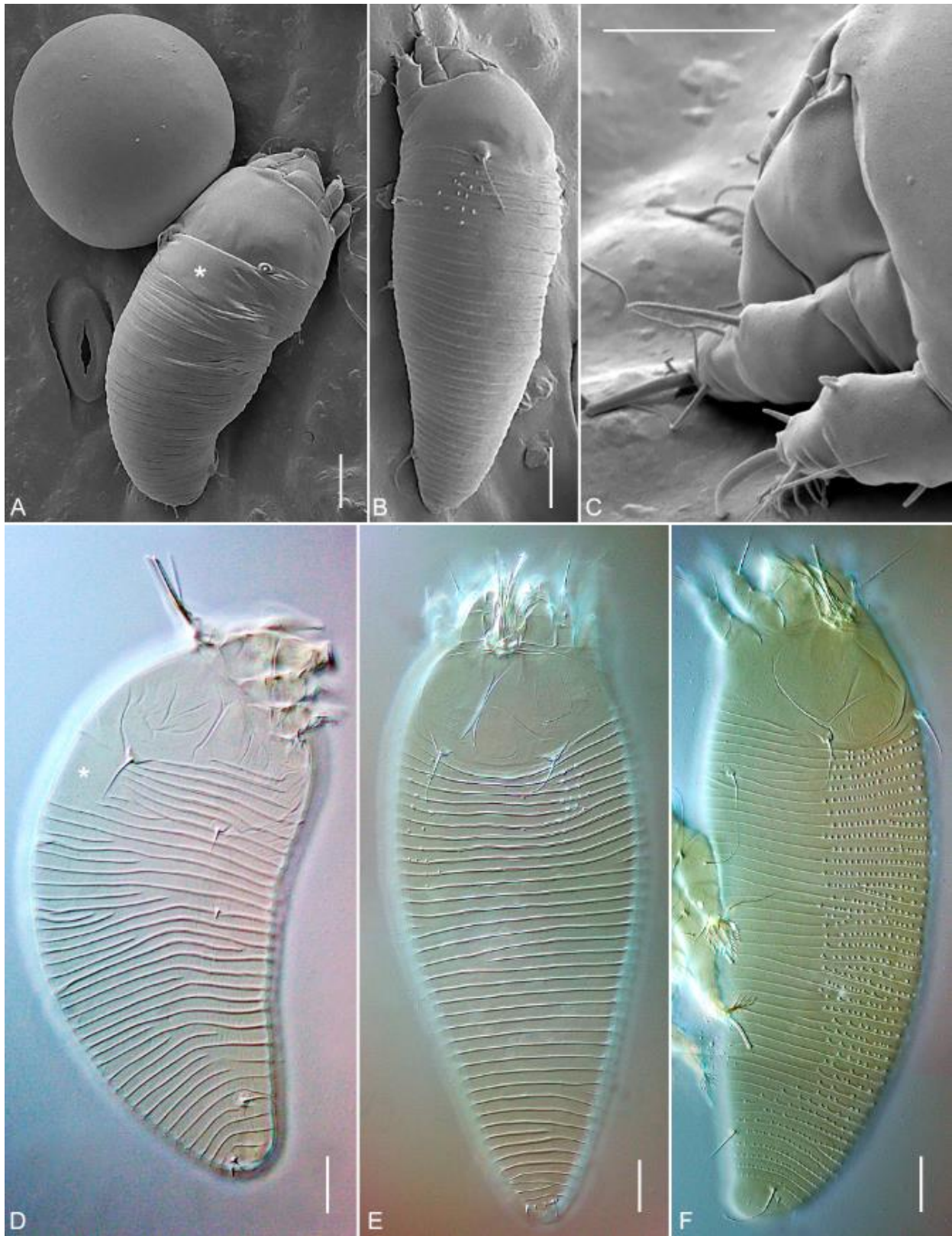


Figure 6. LT-SEM (A–C) and DIC LM (D–F) images of larvae (A,D), morphotype A nymphs (B,C,E) and morphotype B nymph (F) of *Aberoptus schotiae* n. sp. Scale bars: (A,C–F) = 10 μm; (B) = 15 μm. Asterisks indicate cervical pseudotagma.

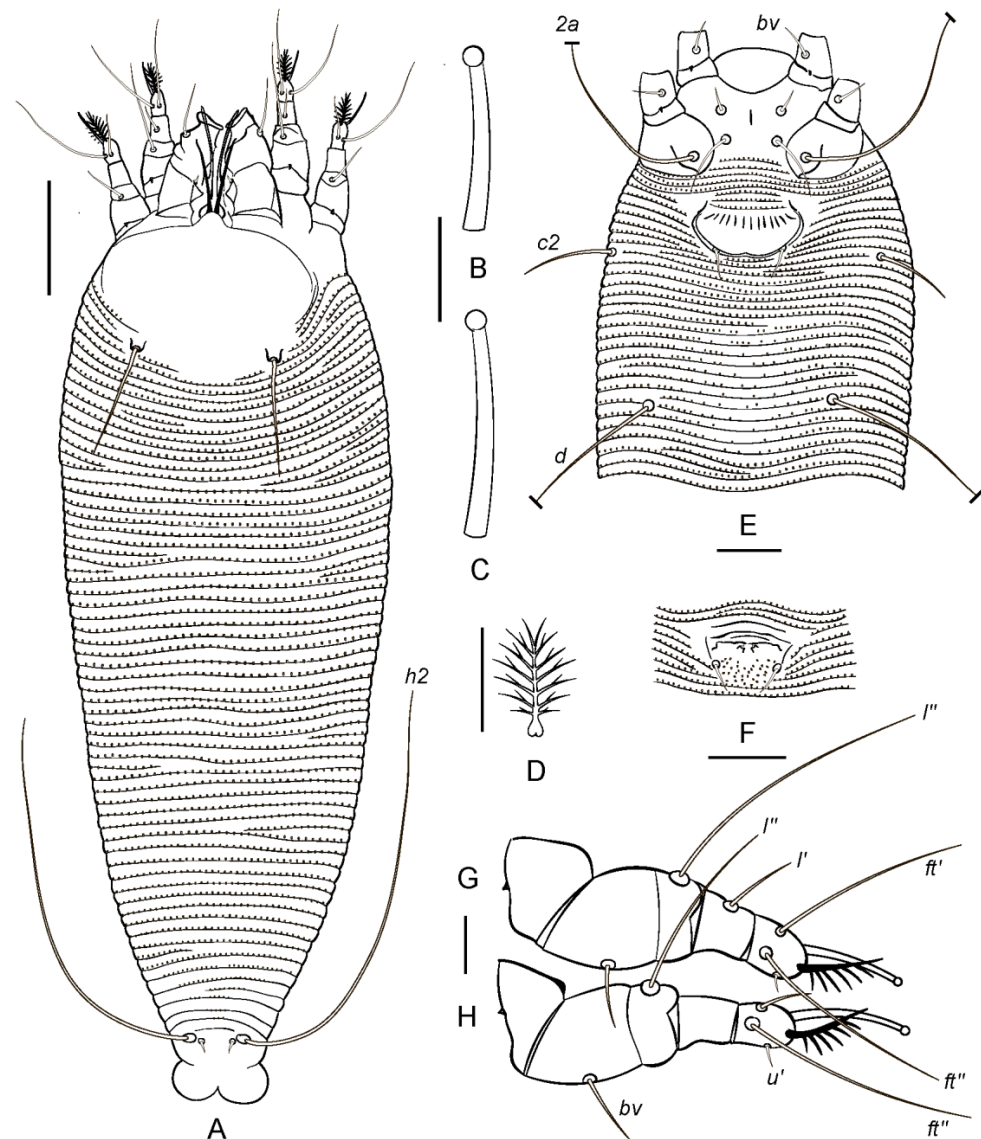


Figure 7. Drawings of female (all except F) and male (F) of *Aberoptus schotiae* n. sp. (morphotype B). (A)—dorsal view of entire female, (B,C)—tarsal solenidia I and II, (D)—empodium I, (E)—female coxigenital area; (F)—male genital area; (G,H)—legs I and II. Scale bar: (A) = 30 μ m; (B–D,G,H) = 5 μ m; (E,F) = 15 μ m.

Gnathosoma directed obliquely down and forward; palps 31 (29–33). Gnathosomal setae: seta v about 0.5; pedipalp genual seta d non-bifurcate, 12 (10–13); pedipalp coxal seta ep 1 (1–2). Suboral plate smooth.

Leg I 31 (27–33), tarsus 5 (4–5), with short terminal spine medial to basis of tarsal solenidion, u' about 0.5, ft' not visible, probably absent, ft'' 19 (18–23), ω 9 (8–10) with small spherical knob; empodium I commonly shaped, 6 (6–7), 4- or (rarely) 5-rayed, all rays except the terminal pair with one additional subray; tibia 6 (5–6) with medioanterior spatulate projection partially covering tarsus, l' 30 (27–34); genu I fused with femur I forming an entire large compound segment, 15 (13–16), l'' 24 (20–28), bv 6 (5–8).

Leg II 25 (24–29), tarsus 3 (3–4), u' 7 (6–8), ft' 10 (9–12), ft'' 23 (18–27), ω 11 (10–12) with small spherical knob; empodium widened, pad-like, 10 (9–11), 11- or 12-rayed, all rays except terminal pair with one tiny process each, additional row of 10–11 short rays on the ventral surface of the empodium; tibia 3 (3–4), weakly separated from tarsus II; genu II fused with femur II forming an entire composite segment, 15 (14–17), l'' 17 (14–19), bv 10 (8–12).

Coxal plates I and II almost smooth, with several faint ridges near tubercles of setae *2a* in some specimens; coxal setae *1b* 4 (3–5), 16 (14–16) apart; *1a* 18 (14–20), 15 (15–17) apart; *2a* 45 (40–58), 38 (36–39) apart. Prosternal apodeme Y-shaped, 3 (2–4) incomplete and one or two complete coxigenital annuli before epigynium. **External genitalia.** Genital coverflap subtriangular, with 6 (6–8) short ridges; 9 (7–9), 24 (23–26) wide; setae *3a* 14 (12–15), 17 (16–18) apart. **Internal genitalia** ($n = 4$). Spermathecae spherical, 4–5 wide; spermathecal tubes short, about 1.5–2 wide, with tiny spermathecal process; longitudinal bridge short, 4–5; anterior genital apodeme trapezoidal, oblique apodeme present.

Opisthosoma dorsally with 56 (54–62) annuli, ventrally with 81 (72–87) annuli between the posterior margin of coxae II and caudal lobes. All annuli microtuberculate except distinct round bald area about 30–40 μm in diameter behind external genitalia and between setae *d*. Setal lengths: *c2* 60 (54–68), *d* 68 (57–73), *e* 33 (26–35), *f* 31 (28–35); *h1* 0.5 (0.5–1); *h2* 4 (2–5); 11 (10–12) annuli from rear shield margin to *c2*; 15 (13–16) annuli between *c2*–*d*; 9 (7–10) annuli between *d* and *e*; 41 (37–43) annuli between *e* and *f*; 5 (5–6) annuli between *f* and *h2*. A well-developed anal secretory apparatus is present and described in detail below in Section 3.3.

GenBank data. OP419490 (D1–D5 28S, isolate A, 1734 bp).

MALE, morphotype A ($n = 5$). Body vermiform, 164–186, 57–62 wide, slightly yellowish. Prodorsal shield smooth, 27–32, 50–58 wide, with small subtriangular frontal lobe, *sc* 26 (21–29), 31 (30–38) apart, directed divergently posteriad. **Leg I** 19–22, tarsus 3–4, *u'* 1–2, *ft'* 0.5–1, *ft''* 10–13, ω 9–11 with small spherical knob; empodium I commonly shaped, 5–6, five-rayed, all rays except the terminal pair with one additional subray; tibia 3–3, commonly shaped, *l'* 5–6; genu I indistinctly separated from femur I, genu+femur slightly swollen, 9–10, *l''* 19–24, *bv* 4–6. **Leg II** 17–21, tarsus 3–3, *u'* 4–5, *ft'* 2–3, *ft''* 12–15, ω slightly curved, directed laterad, 10–12, with small spherical knob; empodium II widened, pad-like, 6–7, seven-rayed, all rays except the terminal pair with one tiny process each, additional row of 6–7 short rays on ventral surface of empodium II; tibia 3–4; genu II fused with femur II forming entire swollen segment 8–10, *l''* 9–10, *bv* 3–4. **Coxal setae** *1b* 2–4, 10–11 apart; *1a* 12–15, 10–11 apart; *2a* 23–28, 26–29 apart, 5–6 coxigenital annuli before genital slit. **Genital area** 14–17, 10–12 wide, setae *3a* 5–7, 9–10 apart, *eu* about 0.5, 2–3 apart, postgenital area (cuticle between *3a*) with rounded microtubercles.

Opisthosoma dorsally with 41–46 annuli, ventrally with 45–55 annuli between posterior margin of coxae II and caudal lobes. All annuli microtuberculate except distinct round area about 20–30 μm in diameter behind external genitalia. Setal lengths: *c2* 22–26, *d* 23–28, *e* 10–13, *f* 19–24; *h1* 0.5–1; *h2* 4–6; 6–8 annuli from rear shield margin to *c2*; 9–12 annuli between *c2*–*d*; 6–7 annuli between *d* and *e*; 20–23 annuli between *e* and *f*; 4–5 annuli between *f* and *h2*. Rudimentary ASA with four short tubes extending up to the 4th telosomal annulus, two small subtriangular medial sacs between them, and a short rectal tube was observed in all studied males.

NYMPH, morphotype A ($n = 5$). Body 186–230, 64–76 wide. Prodorsal shield 32–35, 55–59 wide, with tiny subtriangular frontal lobe, *sc* 9–15. **Leg I** 13–16, all common leg setae present, ω 7–8 with small spherical knob; empodium I commonly shaped, 3–4, five-rayed, all rays except the terminal pair with one additional subray; genu I fused with femur I, swollen. **Leg II** 12–14, all common leg setae present, ω 7–8, with small spherical knob; empodium II widen, pad-like, 5–6, 5-rayed, all rays except terminal pair with one tiny process each, additional row of 4–5 short rays on ventral surface of empodium II, genu II fused with femur II forming entire swollen segment. **Genital area** smooth, setae *3a* 1–2, 10–12 apart. **Opisthosoma** dorsally with 35–42 annuli, ventrally with 32–40 annuli between posterior margin of coxae II and caudal lobes. Opisthosomal annuli smooth except two small groups of 10–20 microtubercles behind setae *sc* at the level where setae *c1* are usually situated in phytoptids. Setal lengths: *c2* 10–13, *d* 10–14, *e* 3–5, *f* 11–14, *h1* about 0.5, *h2* 2–4. ASA non apparent.

Remarks. Four slide-mounted molting nymphs A with partially broken exoskeleton and emerging females of morphotype A were observed. We also observed several notably

swollen slide-mounted nymphs A with broader (but same in number) opisthosomal annuli and containing, almost ready for emerging, adult mite inside. Similar swollen nymphs were observed under SEM. We concluded that they are not a separate immature instar but specimens ready for molting.

LARVA ($n = 5$). Body vermiform, 100–108, 44–49 wide. Prodorsal shield 20–22, 39–43 wide, with tiny subtriangular frontal lobe, *sc* 9–12, 20–23 apart. Prodorsal shield smooth, cuticle of prodorsal shield often wrinkled forming irregular (artificial) lines. Leg I 8–9, leg II 7–8, all common leg setae present, empodia I and II equally shaped, 3-rayed, 3–4. Genital area 7–10, 8–10 wide, two diminutive dot-like setae *3a* present. Opisthosoma dorsally with 31–38 annuli, ventrally with 24–29 annuli, all opisthosomal annuli smooth. Antermost 4–5 opisthosomal annuli fused medially forming a smooth plate (the cervical pseudotagma [57]) 10–12, 20–24 wide. ASA non apparent.

Remarks. Dimorphism of larvae was not observed.

FEMALE, morphotype B ($n = 10$). Body vermiform, with notably broadened bilobed caudal lobe, whitish, 186 (177–193), 67 (65–74) wide at the level of setae *c2*. **Prodorsal shield** subcordate, 37 (34–39), 50 (49–55) wide, with short subtriangular frontal lobe 6 (5–7), 6 (6–8) wide. Prodorsal shield and epicoxal areas smooth. Irregular longitudinal cuticular folds (artificial lines) present in medial part of prodorsal shield in some slightly distorted slide-mounted specimens. Setae *sc* 30 (27–36), 31 (28–33) apart, directed divergently posteriorly. **Gnathosoma** directed obliquely down and forward; palps 25 (24–27). Gnathosomal setae: seta *v* about 0.5; pedipalp genual seta *d* non-bifurcate, 10 (9–13); pedipalp coxal seta *ep* 1 (0.5–1). Suboral plate smooth.

Leg I 26 (24–28), tarsus 5 (4–5), *u'* 4 (4–5), *ft'* 4 (4–5), *ft''* 16 (12–17), ω 9 (8–10) with small spherical knob; empodium I commonly shaped, 6 (6–7), 7-rayed, all rays except the terminal pair with one additional subray; tibia 6 (5–6), *l'* 5 (5–7); genu 4 (4–5), *l''* 30 (29–35), genu and femur distinctly separated; femur 6 (6–7), *bv* 9 (7–10). **Leg II** 24 (22–27), tarsus 5 (4–5), *u'* 4 (4–5), *ft'* 6 (4–7), *ft''* 23 (20–28), ω 9 (8–10) with small spherical knob; empodium II commonly shaped, 7 (6–7), 7-rayed, all rays except the terminal pair with one additional subray; tibia 4 (4–5); genu 4 (3–5), *l''* 12 (10–15), genu and femur distinctly separated, femur 8 (6–8), *bv* 9 (7–10).

Coxal plates I and II almost smooth, with several faint ridges near tubercles of *2a* in some specimens; coxal setae *1b* 6 (4–7), 14 (13–16) apart; *1a* 30 (25–37), 12 (11–14) apart; *2a* 64 (55–69), 25 (23–26) apart. Prosternal apodeme short, 3 (2–4) incomplete and two or three complete coxigenital annuli before epigynium. **External genitalia.** Genital coverflap subtriangular, rounded posteriorly, with 10 (9–11) short longitudinal ridges; 9 (8–10), 25 (23–27) wide; setae *3a* 15 (12–16), 15 (14–16) apart.

Opisthosoma dorsally with 58 (53–64) annuli, ventrally with 68 (61–72) annuli between posterior margin of coxae II and caudal lobes. All annuli microtuberculate except indistinct round area about 20–25 μm in diameter between tubercles of setae *d* bearing very sparse small microtubercles or almost smooth/bald. Setal lengths: *c2* 20 (18–26), *d* 80 (63–84), *e* 64 (54–68), *f* 30 (26–33); *h1* 3 (2–3); *h2* 79 (63–84); 11 (10–12) annuli from rear shield margin to *c2*; 14 (13–15) annuli between *c2*–*d*; 15 (13–16) annuli between *d* and *e*; 22 (20–23) annuli between *e* and *f*; 5 (5–6) annuli between *f* and *h2*. Rudimentary paired tubes and indistinct medial sac of ASA present in all studied specimens.

GenBank data. OP419491 (D1–D5 28S, isolate B, 1700 bp).

MALE, morphotype B ($n = 5$). Body vermiform, 154–161, 54–59 wide, whitish. Prodorsal shield smooth, 26–33, 43–47 wide, with small subtriangular frontal lobe, *sc* 28 (26–34), 33 (32–36) apart, directed divergently posteriorly. **Leg I** 19–21, tarsus 4–5, *u'* 3–4, *ft'* 6–9, *ft''* 14–17, ω 9–10 with small spherical knob; empodium I commonly shaped, 5–7, 6-rayed, all rays except terminal pair with one additional subray; tibia 3–4, commonly shaped, *l'* 4–5; genu 3–4, *l''* 21–25, femur 6–8, *bv* 5–7. **Leg II** 19–20, tarsus 4–5, *u'* 3–4, *ft'* 3–4, *ft''* 13–19, ω 8–9 with small spherical knob; empodium I commonly shaped, 6–7, 6-rayed, all rays except terminal pair with one additional subray; tibia 3–4, commonly shaped; genu 3–4, *l''* 9–12, femur 6–7, *bv* 5–6. **Coxal setae** *1b* 3–4, 10–11 apart; *1a* 14–17, 10–11 apart; *2a* 28–39,

24–28 apart, 5–6 coxigenital annuli before genital slit. **Genital area** 10–12, 15–17 wide, setae *3a* 5–7, 10–13 apart, *eu* about 0.5, 2–3 apart, postgenital area (cuticle between *3a*) with rounded microtubercles.

Opisthosoma dorsally with 43–50 annuli, ventrally with 47–56 annuli between posterior margin of coxae II and caudal lobes. All annuli microtuberculate except round area about 15 µm in diameter behind external genitalia with sparse or no microtubercles. Setal lengths: *c2* 14–18, *d* 36–43, *e* 35–41, *f* 19–23; *h1* 2–4; *h2* 44–52; 6–7 annuli from rear shield margin to *c2*; 8–10 annuli between *c2*–*d*; 10–12 annuli between *d* and *e*; 18–21 annuli between *e* and *f*; 5–6 annuli between *f* and *h2*. Rudimentary ASA similarly shaped as in females of the morphotype B was observed in all studied males.

NYMPH, morphotype B (n = 4). Body 150–162, 55–60 wide. Prodorsal shield 30–33, 38–42 wide, with tiny subtriangular frontal lobe, *sc* 10–13. **Leg I** 13–17, all common leg setae present, ω 5–6 with small spherical knob; empodium I commonly shaped, 5–6, 5-rayed, all rays except the terminal pair with one additional subray; genu and femur indistinctly separated. **Leg II** 13–16, all common leg setae present, ω 5–6 with small spherical knob; empodium I commonly shaped, 5–6, 5-rayed, all rays except the terminal pair with one additional subray; genu and femur indistinctly separated. **Genital area** smooth, setae *3a* 2–3, 9–10 apart. **Opisthosoma** dorsally with 40–46 annuli, ventrally with 38–44 annuli between posterior margin of coxae II and caudal lobes. All dorsal annuli microtuberculate, ventral annuli smooth except 9–10 posteriormost annuli with microtubercles. Setal lengths: *c2* 7–11, *d* 22–28, *e* 9–12, *f* 12–15, *h1* 2–3, *h2* 22–29. ASA not apparent.

Remarks. One nymph B molting into a female B was observed in slides.

Type material. Holotype female from slide E95, paratype females, males, nymphs, and larvae in slide series E96 and E97 collected on 20 November 2013 by P. Chetverikov and C. Craemer in Pretoria, South Africa (−25.711997, 28.227131) from under silk mats on the lower leaf surface of *Schotia brachypetala* Sond. (Fabaceae). Type material is deposited in the Acarological Collection of the Zoological Institute of the Russian Academy of Science (ZIN RAS) in Saint-Petersburg (Russia) and ARC Plant Protection Research Institute in Roodeplaat, Pretoria (South Africa).

Host and relation to host. Mites live under thin silk mats that they produce along and between veins, usually on lower and rarely on upper leaf surfaces of *Schotia brachypetala* Sond. (Fabaceae).

Additional material. Adults and immatures in slide series E102–E107 (13 March 2013), in slide series E3667–E3669 (9 April 2015), in vials #1189 (15 March 2013), #1295–#1297 (28 November 2016), and #M188–#M189 (2 November 2017) filled with 96% ethanol—all of them were collected from the type locality, by the same collectors, from the same host plant and relation to host.

Etymology. The species name, *schotiae*, is a noun, gender feminine, in genitive case. It is derived from the generic name of the host plant, *Schotia*.

Differential diagnosis. Adults of the new species are most similar to those of *Aberoptus cerostructor* Flechtmann 2001. Web-spinning females of *A. schotiae* n. sp. have genital coverflap with 6–8 short longitudinal ridges (smooth in *A. cerostructor*) and a “spot” of ventral cuticle behind the external genitalia, devoid of microtubercles (the “spot” is indistinct and formed by longer and denser microtubercles in *A. cerostructor*). Non-spinning females of *A. schotiae* n. sp. have smooth prodorsal shield (seven longitudinal lines in *A. cerostructor*), indistinct “spot” on ventral annuli with sparse microtubercles (“spot” absent in *A. cerostructor*), and uniformly microtuberculate ventrolateral opisthosomal annuli (two distinct lateral “bands” of the smooth cuticle lateral to setae *c2* and *d* in *A. cerostructor*).

3.2. Field Observations and Seasonal Distribution of Morphotypes A and B in Samples

In Pretoria, South Africa, the summers are relatively warm and long, continuing for almost six months (October–March). June and July are the coldest months (winter), preceded by a short autumn (April and May) and followed by a short spring (August and

September). Relative humidity in Pretoria varies from about 45% to 60%. July, August, and September are the driest months (Figure 8). Climatically, a year in Pretoria may be roughly divided into two periods: warm-humid and cool-dry. All our samples of *A. schotiae* n. sp. were collected at the end and at the beginning of the warm-humid period in 2013–2017 (black dots in Figure 8).

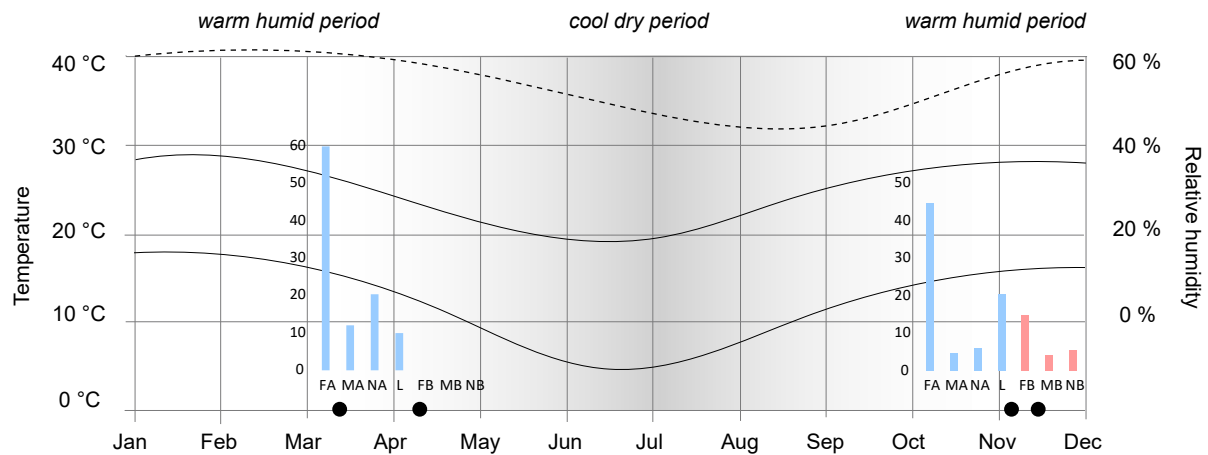


Figure 8. Climatic characteristics of the type locality of *Aberoptus schotiae* n. sp. and abundance (%) of the morphotypes A (blue) and B (pink) in the samples collected in 2013–2017 in South Africa. Average relative humidity (dotted line), minimum (lower solid line), and maximum (upper solid line) temperature in Pretoria depicted, based on data from <https://weather-and-climate.com> (accessed on 22 September 2022). Notations: L—larvi; FA, MA, NA, FB, MB, NB—females (F), males (M), and nymphs (N) of morphotypes A and B. The area marked by gray gradient indicates the cool-dry period of the year in Pretoria.

During SEM sessions, which were all undertaken in February 2003 (5, 10, and 19 February), morphotype B was not registered. At the end of the warm-humid period (March and April), only morphotype A was found. We did not sample mites during the cool-dry period. On the old leaves collected in early November (the first half of the warm-humid period), we found many empty, large old nests, sometimes covering about 50% of leaves, with no mites; as well as, on the younger leaves, small new nests with several web-spinning females A, numerous eggs and immatures (larvae and nymphs A). In the middle and late November, adults and immatures of both morphotypes A and B were found in the samples. In November, we observed many small neighboring web nests adjacent to larger nests (Figure 1F), creating the impression that the smaller nests coalesced and formed larger nests.

Under stereomicroscope in laboratory conditions, we observed large yellowish females with elongated tapered telosomes (characteristic of morphotype A) spinning the web above themselves via bending and moving the caudal part of their opisthosomas many times. Smaller mites possessing more obtuse or blunt anal lobes (morphotype B) were not observed spinning. Morphotype A was present in all our samples and was always the most abundant (Figure 8). Morphotype B was registered only in November (about 23% of the total abundance). During this month, males and nymphs of morphotypes A and B were notably sparser than larvae, and the ratio of A/B females was approximately 3:1. The abundance of larvae in samples collected in November and December was two times higher (20%) than in March and April (9%), indicating a difference in the intensity of reproduction.

3.3. Web-Spinning in *Aberoptus schotiae* n. sp.

3.3.1. Web Structure and Appearance

Under SEM, a new nest produced by a single female (morphotype A) consisted of thin silk threads resembling irregular netting and covering a semicircular area of about 70–80 μm in diameter (Figure 9A). The threads were apparently anchored to the plant surface. At a later stage, nests resembled more solid, thin fabric-like sheets or plates (Figure 9B), possibly due to the consolidation of silk threads or chemical transformation of the silk exposed to external elements and/or depositing of a matrix. Under stereomicroscope LM, the new web looked dull and gray, whereas the mature or older web was whitish and glossy. Neighboring nests produced by different females merged with each other forming a larger web mat. Atomic Force Microscopy indicated that a mature web mat consists of filaments and a matrix (Figure 9C–H). The filaments were arranged randomly, intertwined in all directions, and had a thickness from 50 to 500 nm; occasionally, there were filaments of 1 μm thick. The matrix is an amorphous substance, sometimes forming clusters in the form of globules of various sizes.

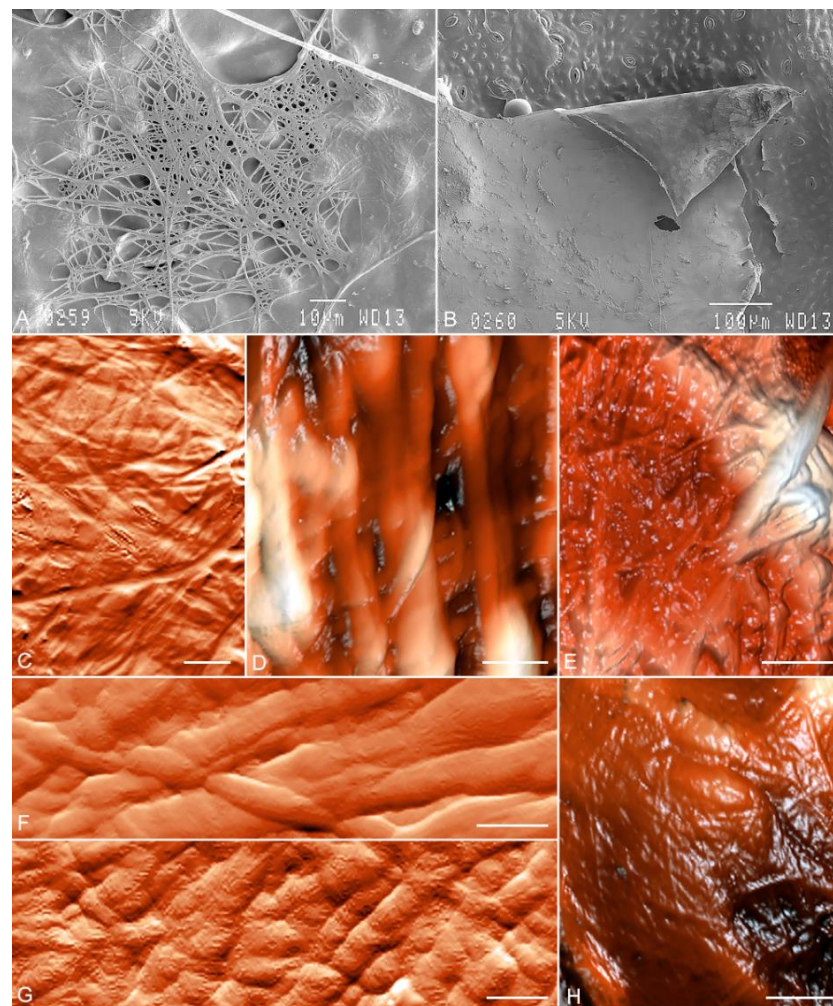


Figure 9. LT-SEM images (A,B) and AFM topographical scans (C–H) of young (A) and mature (B–H) web produced by *Aberoptus schotiae* n. sp. Scale bar: (A) = 10 μm ; (B) = 100 μm ; (C–G) = 1 μm ; (H) = 5 μm .

3.3.2. Silk Producing Anal Secretory Apparatus (ASA) of Web-Spinning Females of *Aberoptus schotiae* n. sp.

In females of morphotype A of *A. schotiae* n. sp. the ASA is situated in the caudal part of the opisthosoma and consists of two pairs of silk-secreting anal glands with bifurcated

ducts, three cuticular sacs (dorsal, medial, and ventral), and a topographically complex rectal tube functioning as an excretory channel (Figures 10–13). The anal glands were revealed with LMSSS and TEM (Figures 11 and 12). Each of the four anal glands is formed by elongated cells. These cells partially wrap each other, forming a layered tissue resembling puff pastry with distinct intercellular lacunas converging toward the gland duct. The anal gland cells have well-developed endoplasmic reticula concentrated under the cell membrane, numerous mitochondria, and large vesicles (Figure 12C,D).

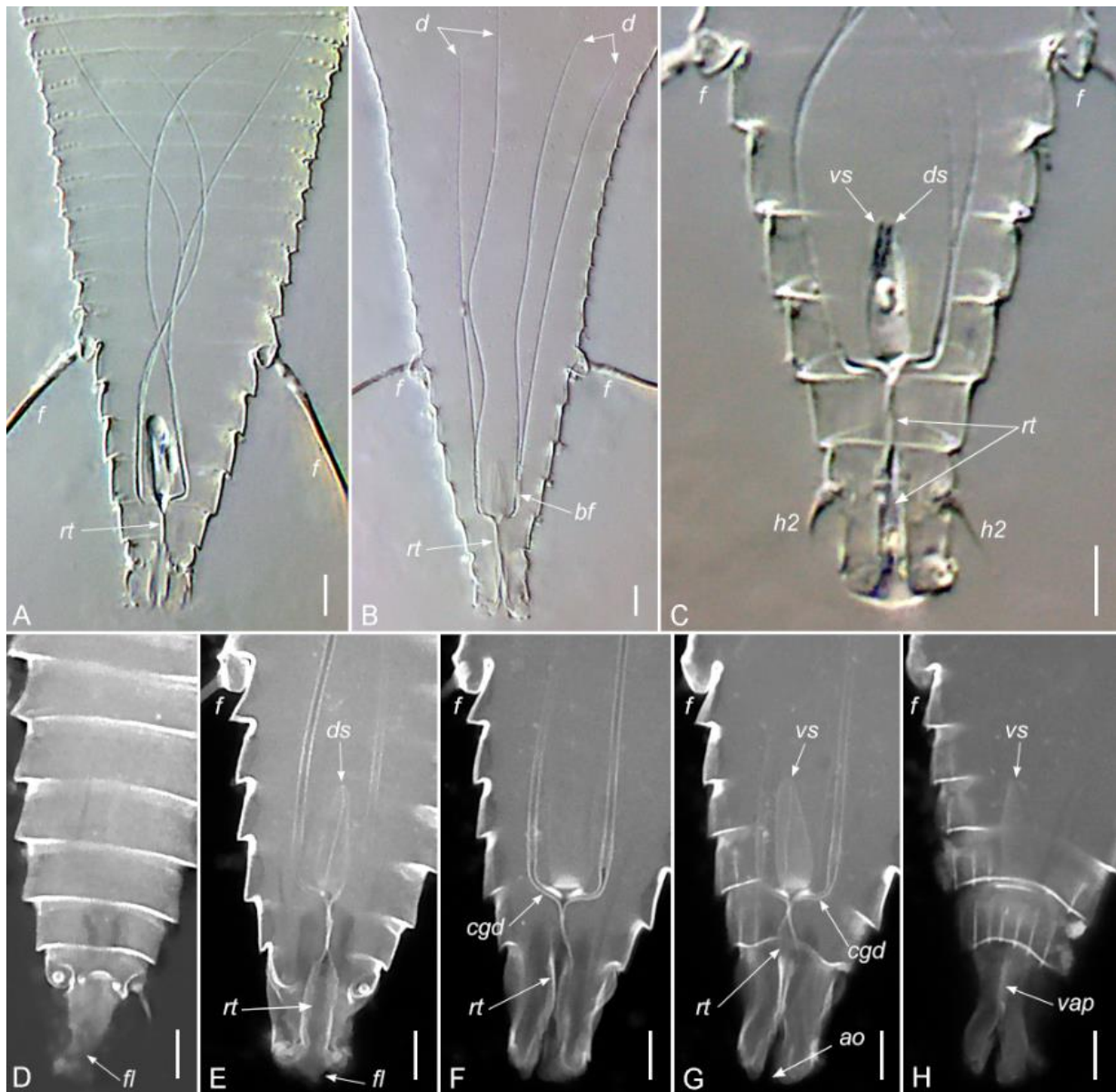


Figure 10. DIC LM (A–C) and CLSM images ((D–H), microphotographs with gradually increasing depth of focus showing cuticle-lined elements of anal secretory apparatus in *Aberoptus schotiae* n. sp. Scale bar = 2 μ m. Notations: *ao*—anal opening, *bf*—bifurcation of common gland duct, *d*—gland duct, *cgd*—common gland duct, *f*—seta *f*, *fl*—flap, *h2*—seta *h2*, *ds*—dorsal sac, *vs*—ventral sac, *rt*—rectal tube, *vap*—ventral apodeme.

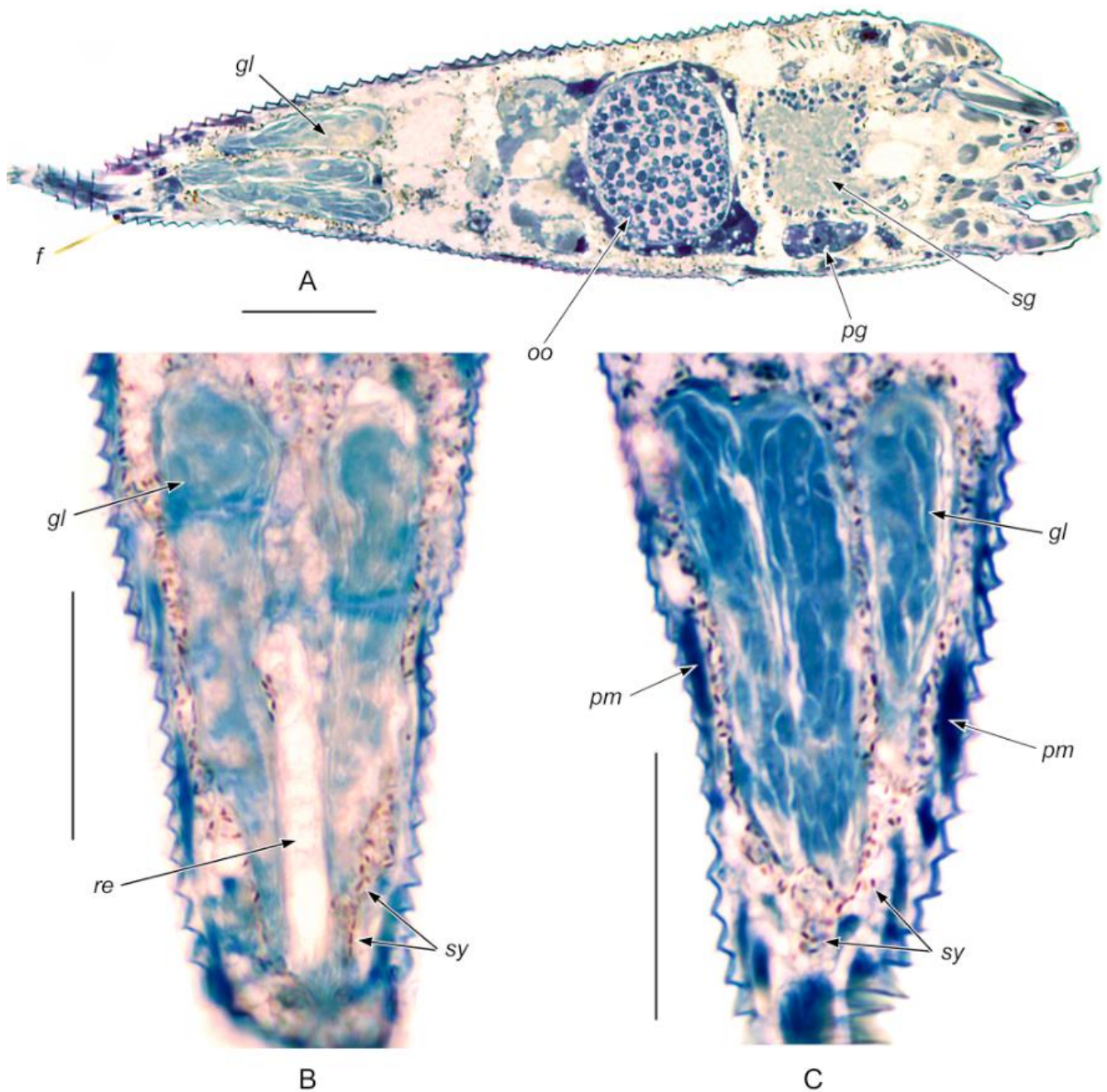


Figure 11. Frontal semi-thin sections of *Aberoptus schotiae* n. sp. (LMSSS). (A)—entire mite in dorsoventral position, (B,C)—caudal part of opisthosoma containing silk-producing anal secretory apparatus. Notations: *f*—opisthosomal seta *f*, *gl*—silk gland, *re*—anterior part of rectum, *oo*—oocyte, *pg*—paired gland, *pm*—peripheral muscles, *sg*—synganglion, *sy*—symbiotic bacteria. Scale bars: (A) = 30 μ m; (B,C) = 20 μ m.

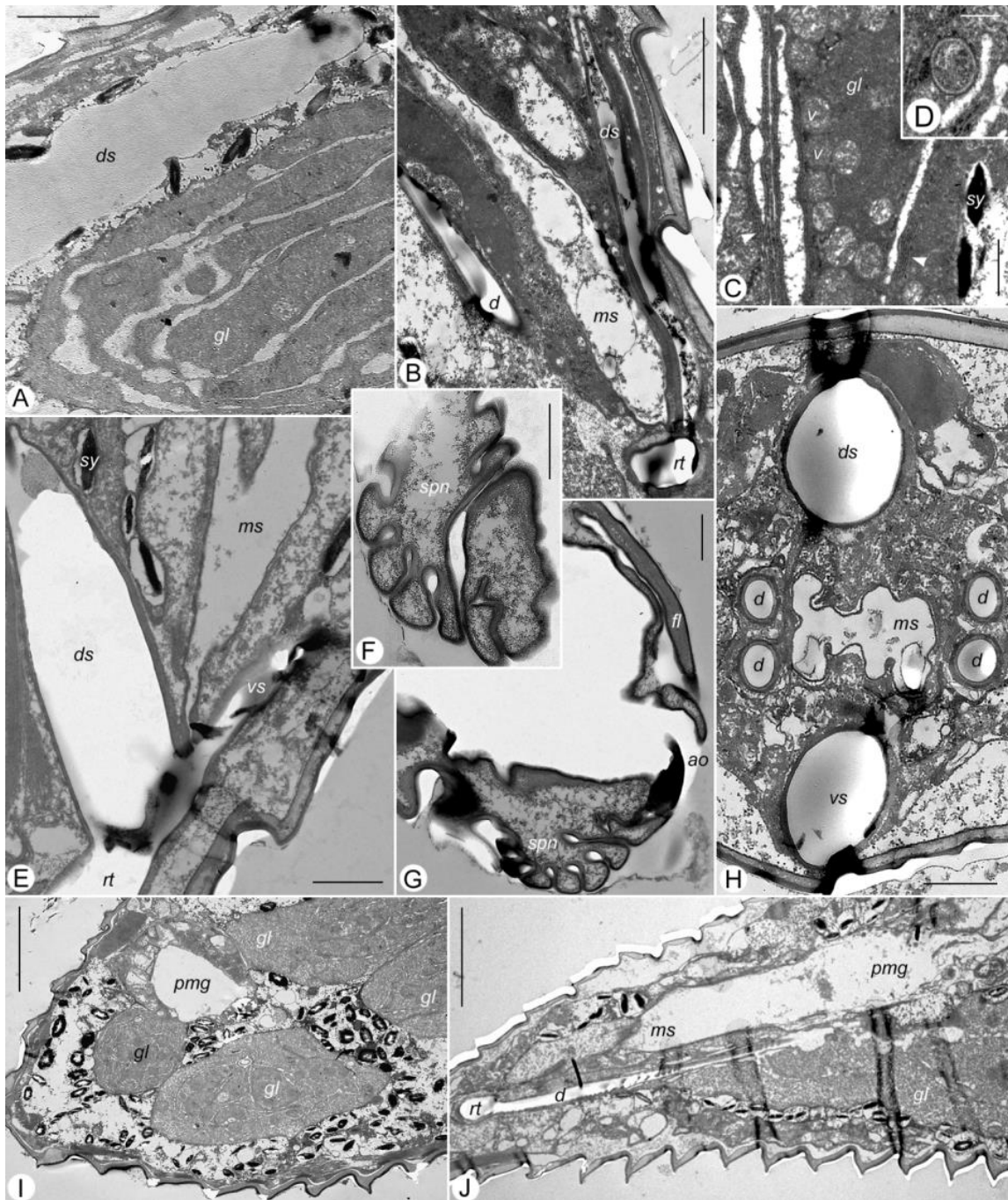


Figure 12. Transmission electron micrographs of caudal body region of web-spinning females of *Aberoptus schotiae* n. sp. (A)—dorsal sac and anal gland, (B)—oblique section at the level where common gland duct and sacs join rectal tube, (C,D)—vesicles (C) and mitochondria (D) in the cell of anal gland (arrowheads in Figure 12C indicate endoplasmic reticulum), (E)—junction area of rectal tube and three sacs, (F)—cross section of spinneret, (G)—spinneret, anal opening, and cuticular flap, (H)—frontal section at the level of the third telosomal annulus, (I)—four anal glands and putative posterior midgut displaced towards dorsal cuticle, (J)—longitudinal section through region of transition between medial sac and putative posterior midgut. Notations: *ao*—anal opening, *d*—duct of anal gland, *ds*—dorsal sac, *fl*—cuticular flap, *gl*—anal gland, *ms*—medial sac, *pmg*—putative posterior midgut, *rt*—rectal tube, *spn*—spinneret, *sy*—symbiotic bacteria, *v*—vesicles, *vs*—ventral sac. Scale bars: (A,B) = 2 μ m; (C,E,H) = 1 μ m; (D) = 0.25 μ m; (F,G) = 0.5 μ m; (I,J)—5 μ m.

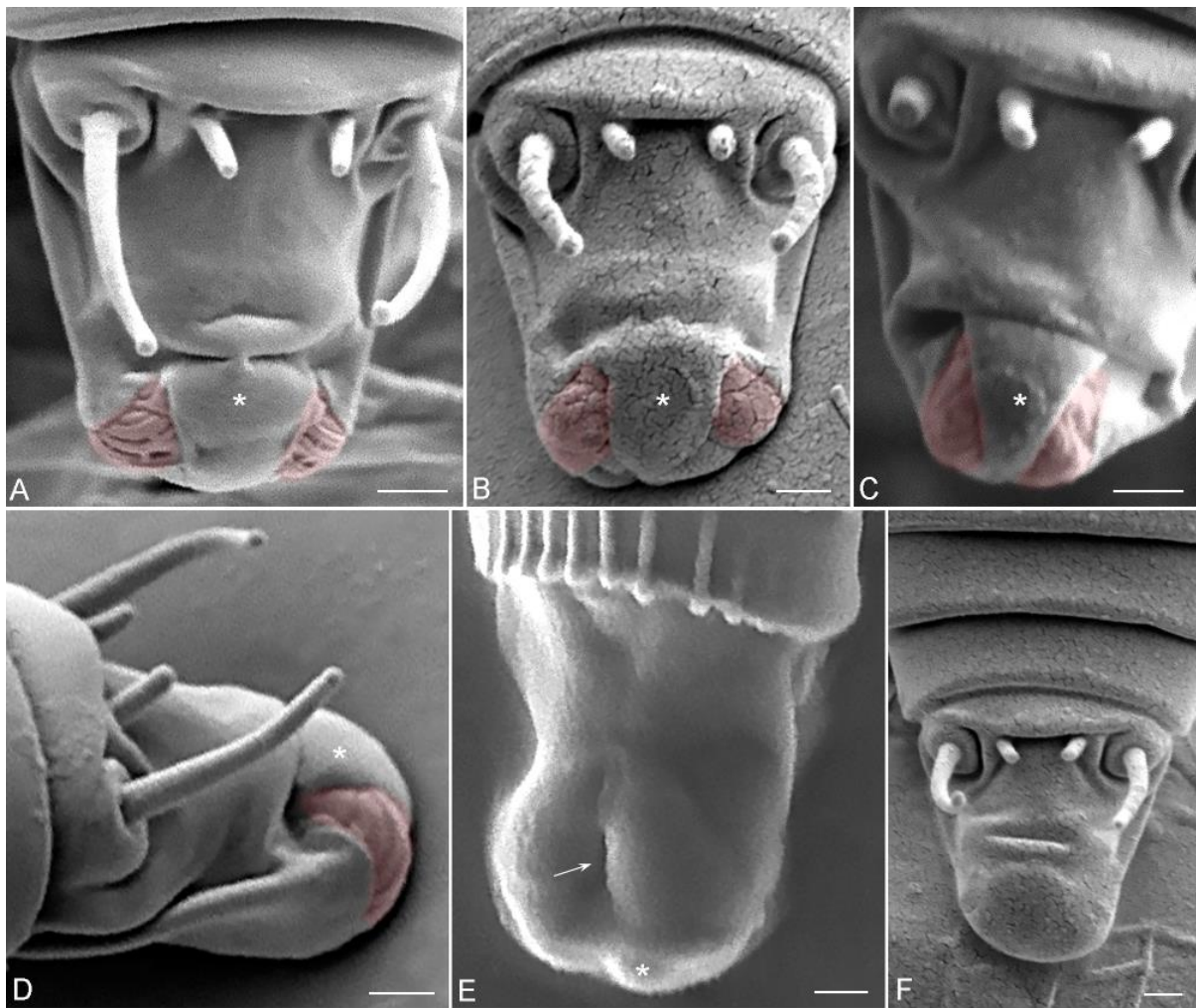


Figure 13. LT-SEM images of caudal lobes in five females (A–E) and male (F) of morphotype A of *Aberoptus schotiae* n. sp. (A,B,C,F)—dorsal view; (D)—lateral view; (E)—ventral view, arrow indicates putative anal opening. Asterisks indicate cuticular flap. Areas of porose cuticle (the spinneret) colored red. Scale bars = 1 µm.

The secretions of the glands drain through the ducts into the rectum and apparently accumulate in the sacs (Figures 10 and 12B). The gland ducts begin from the proximal rectal tube at the level of the second telosomal annulus from the rear as entire and is termed here as common gland ducts (CGD). The left and right CGD have a sharp curve. In this curved area, each of them forks into two branches that extend antieriad to the level of 15–20 caudal opisthosomal annulus (Figure 10).

The dorsal (DS) and ventral (VS) sacs are equally sized, pear-shaped cuticular reservoirs, notably wider basally and narrow apically (Figures 10 and 12). In laterally viewed specimens, they are positioned one above the other (in the sagittal plane) at the level of the posterior-most 3–5 telosomal annuli. At the level of the second telosomal annulus from the rear, DS and VS are widely connected with the rectal tube (Figure 12E) and appear to be its direct dorsal and ventral continuations. Both sacs were filled with homogenous electron-lucent material (putative silk) under TEM (Figure 12A). They had a constant size in all investigated specimens and thick cuticular walls, suggesting that they did not stretch much.

The medial sac (MS) is located between the glands. It occupies a central or median position in transverse (Figure 12H) or longitudinal (Figure 12J) cross sections, respectively. The presence of the inner cuticular lining (Figure 12B,H) suggests that the MS is the

anterior segment of the hindgut homologous to the rectal sac *sensu* [18]. The MS is three to four times longer than the VS and DS, filled with an amorphous matrix usually containing large bubbles, and has thinner cuticular walls forming internal protuberances. Caudally the MS joins the rectal tube with a very thin duct about 1 μm long and 0.05 μm in diameter (Figure 12E). Anteriorly the MS continues into a wide tubular structure devoid of cuticular lining and is interpreted here as the posterior midgut (Figure 12I,J).

The rectal tube (RT) is a thick-walled cuticular structure occupying the space of one to two posterior-most opisthosomal annuli and the space between the anal (caudal) lobes (Figure 10E). It is notably wider under the dorsal cuticle (Figure 10E vs. Figure 10G). Ventrally, it narrows and forms a short, longitudinally folded, ridge-shaped apodeme (Figure 10H). In the posterior half, the inner surface of the RT is grooved. The RT grooves continue into canaliculi that open externally in two lateral areas of the porose cuticle and form the spinnerets (Figure 12F,G and Figure 13). In males of morphotype A investigated under LT-SEM, the spinnerets were not observed (Figure 13F). The anal opening is situated between terminal cuticular folds of the opisthosomal caudal lobe and is covered dorsally with a thin subtriangular cuticular flap (Figures 12G and 13, asterisk).

Under LT-SEM, we observed web-spinning females with their caudal lobes in two positions. In position I (Figure 13A–D), the telosome is constricted, the anal lobe is invaginated, and the anal opening is tightly covered with the flap; therefore, only the two areas of porose cuticle may function for the slow excretion of the contents of the rectal tube in the form of thin threads. In position II (Figure 13E), the telosome is narrowed and elongated (maybe relaxed), the anal lobes are protrudent, and the anal opening is exposed and may function for faster emptying of the rectal tube.

Similar to our previous TEM study of a gall mite *Fragariocoptes setiger* (Nalepa 1894) [27], we observed symbiotic bacteria irregularly distributed between all internal organs. They were especially numerous in the extracellular spaces between parenchymal cells and around the ovarium and silk glands (Figure 11B,C and Figure 12C,E,I). LMSSS and TEM of *A. schotiae* n. sp. also revealed the general internal anatomy of Eriophyoidea [18], including a large central nervous system, paired glands, bundles of peripheral muscles, a series of oocytes at different developmental stages, and large parenchymatous cells filling the space between internal organs (Figure 11).

3.4. Molecular Phylogenetics

3.4.1. GenBank Data and 28S Sequence Diversity

D1–D5 28S sequences of *Aberoptus schotiae* n. sp. females of morphotypes A (OP419490) and B (OP419491) are identical (K2P distance = 0.000%), except three sites in D1 (Y/Y) and D2 S/C,Y/T) regions. A BLAST search for these two 28S sequences against Eriophyoidea returned as the best hit the sequence KT070266 (*Aberoptus platessoides*, 56% coverage, 88.37% identity), when filtered by coverage (>40%) and sorted by E-value. The analysis of sequence diversity revealed distinct dissimilarity between sequences OP419490 and OP419491 of *Aberoptus schotiae* n. sp. and sequence KT070266 of *A. platessoides* (K2P distance = 11.6% and 11.5% correspondingly), confirming species distinction.

3.4.2. Molecular Phylogenetic Analyses (Figure 14)

Our analyses produced a partially resolved tree of Eriophyoidea and revealed several large well-supported clades (Figure 14). The genus *Aceria* was inferred paraphyletic, with members of this genus scattered in different large clades. Genera of the web-spinning mites, *Aberoptus* and *Cisaberoptus*, do not form a monophyletic group but belong to different distantly related clades I and II. Genus *Aberoptus* was inferred monophyletic and basal in clade I comprising members of different genera of the tribes Aceriini and Anthocoptini. These two tribes possess setae *sc* directed backward. Genus *Cisaberoptus* belongs to a taxonomically divergent clade II, most members of which (except two) belong to the tribes characterized by setae *sc* directed up or forward (Phyllocoptini, Eriophyini, and Calacarini).

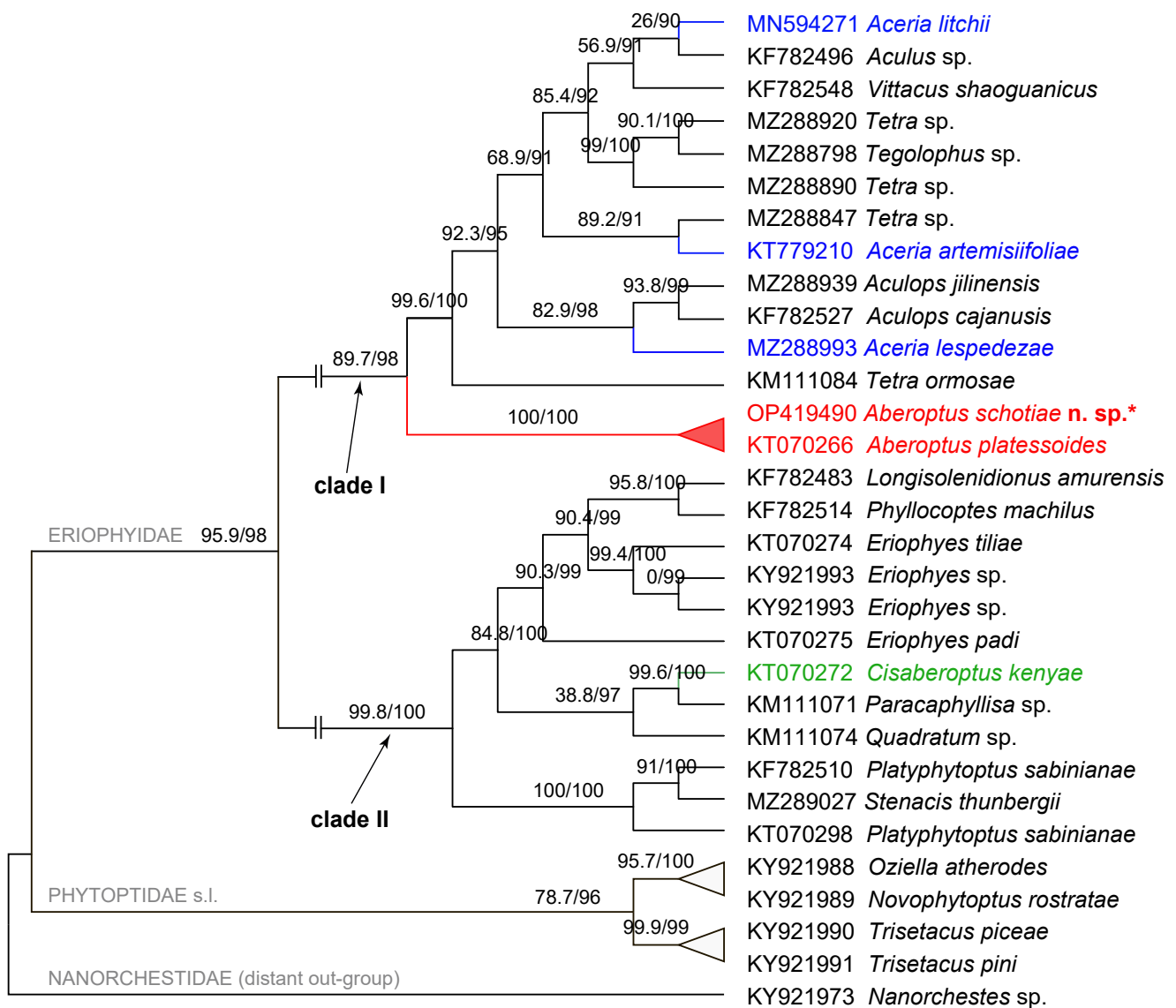


Figure 14. Maximum likelihood tree of Eriophyoidea based on a nucleotide alignment of the D1–D2 regions of 28S gene showing position of the web-spinning mites (colored red and green). Only clades I and II including sequences of *Aberoptus* and *Cisaberoptus* are shown; all other clades are omitted (//). Branches are labeled by UF bootstrap support (UFBS), preceded by values of approximate likelihood-ratio test (SH-aLRT). Members of the genus *Aceria* from clade I are colored blue. Asterisk indicates the new sequence obtained in this study.

4. Discussion

Conspicuity and seasonal distribution of *Aberoptus* morphotypes. The synchronous or asynchronous presence of alternative phenotypes occupying the same habit is typical for various taxa of arthropods, including acariform mites [58–60]. Examples of female and, rarely, male dimorphism have been reported in all major phylogenetic lineages of Eriophyoidea [61], and a complex life cycle assuming female dimorphism was hypothesized to be symplesiotypic of contemporary Eriophyoidea [62,63]. Morphological dimorphism in eriophyoids can be almost indistinguishable or, otherwise, so pronounced that different forms of the same species could have characteristics of different genera [28], and then only laborious life cycle reconstructions or DNA barcoding can prove morphotype conspicuity [64–66].

Genus *Aberoptus* is a clear example of an eriophyoid taxon possessing a complex life cycle and pronounced the same sexual and bisexual morphological dimorphism. Here, we described two morphotypes (A and B) of females, males, and nymphs and one morphotype of larvae of a new web-spinning species, *A. schotiae* n. sp. DNA barcoding showed that females of different morphotypes have identical sequences of the 28S gene, which indicates their conspecificity. All studied larvae of *A. schotiae* n. sp. are homomorphic and, contrary to all other instars, possess cervical pseudotagma. Rarely, this pseudotagma is present in adults of some Eriophyidae and presumably corresponds to the suppressed metapodosomal segments [57,67]. There are no data on larvae of other *Aberoptus* spp. to conclude if all of them have this pseudotagma or not.

Contrary to tetranychoids of which both sexes contribute to spinning the web nests [68], in *A. schotiae* n. sp. (and probably in the whole genus *Aberoptus*), only females of one morphotype are web-spinning. Our incomplete seasonal data indicate that the web-spinning morphotype A might persist on plants most of the year, unlike the non-spinning morphotype B which is present in populations for a notably shorter time and in fewer numbers. The non-spinning morphotype B can be found in nests from November, but might have already disappeared by February. Different morphotypes of two Brazilian *Aberoptus* spp. coexist in November (*A. cerostructor*) and in April (*A. inusitatus*) and, similar to *A. schotiae* n. sp., the web-spinning females are more numerous in all samples than non-spinning, although in different proportions [33,38]. The variations of the A/B morphotype ratio probably depend on annual climate fluctuations in particular geographical regions.

Morphological dimorphism in *Aberoptus*. Female dimorphism in Eriophyoidea typically includes differences in body shape, size and color, the distinctiveness of prodorsal shield ornamentation, microtuberculation and the number of opisthosomal annuli, and morphology of empodia [61,65,69]. In *A. schotiae* n. sp., a series of unique morphological structures have evolved in morphotype A as a putative adaptation to web-spinning. Their heteromorphic empodia, laterally directed tarsal solenidia, spatulate processes, and stout legs with femoro-genua consolidation assist in stabilizing the prosoma during spinning. The large ventral bald “spot” of the postgenital cuticle is a highly flexible area, allowing sharp bending of the body. The elongated, tapered caudal part of opisthosoma, bearing rudimentary setae *h1* and *h2* and containing the spinnerets and a hypertrophied ASA, function as a specialized “web-spinning machine”.

Non-spinning morphotype B of *A. schotiae* n. sp., similar to the correspondent morphotypes in *A. inusitatus* and *A. cerostructor*, looks like a typical *Aceria* with a broad, blunt caudal lobe and notably longer caudal setae *h2*. Britto et al. [33] showed that morphotype B of *A. inusitatus* survived only under the web and concluded that web-spinning morphotype A is a migratory form. Long opisthosomal setae, including *h2*, are traditionally considered to assist in dispersal by wind ([24] and [70], p.348), the main mode of dispersal in eriophyoids [71]. It is not clear why setae *h2* are so well developed in morphotype B (other than a possible atavism, reversion, or retention of an ancestral attribute [72]), although their shortening in morphotype A is evident: otherwise, they would get tangled with silk threads. Modeling the biomechanics of eriophyoid aerial dispersal, including estimation of the role of opisthosomal setae *h2* in the “mite flight” could clarify the intermorphotype differences in *h2* length.

Function of epicoxal setae in Eriophyoidea. LTSEM indicates the direction of palpcoxal setae *ep* and the distance between their tips varies among specimens of *A. schotiae* n. sp. They can be directed convergently up, touch each other or be almost appressed to the dorsal surface of basal chelicerae (Figure 4H,I,J). Setae *ep* could be a receptor detecting the degree of compression of palps and position of chelicerae during feeding. This important function possibly explains why in eriophyoids, “... the palpcoxal seta is so surprisingly well developed, compared to ... other mites” [24].

Web function and web-spinning mechanism in *Aberoptus*. Webbing plays an important role in *Aberoptus* ecology. Managing the micro-environment on a host plant and protection from predators and pathogenic fungi are the most apparent web functions in

Aberoptus and other web-spinning taxa of Eriophyoidea. It could also serve for occupying the maximal area of the leaf and isolating the food source from sympatric competitors, e.g., other eriophyoids (and unrelated mites like tarsonemids) associated with the same host plant and non-adapted for living under the web.

In *A. schotiae* n. sp., the webs of different ages look different (Figure 9A,B). The transformation of the net-like young web into an older plate-like mat could be explained by the ability of silk threads to consolidate. An alternative hypothesis implies that a mite first makes a frame (young web) and then excretes a liquid matrix rapidly hardening in air. The latter agrees with our LTSEM observation if assumed that thin silk threads are excreted via the two spinnerets when the anal opening is covered by the subtriangular cuticle flap, and the caudal lobe is invaginated due to the muscle constriction (position I). In the relaxed state, the caudal lobe is elongated (position II), and the matrix can be excreted through the opened rectal tube.

Homology of ASA in Eriophyoidea. In males of morphotype A and both sexes of morphotype B of *A. schotiae* n. sp., the ASA is weakly but at the same degree developed and similarly structured as in other non-related eriophyoids in which an ASA has been recently reported [19,41–43]. In these eriophyoids, silk production is highly probable, although in much smaller quantities than in the web-spinning females of *Aberoptus*. The wide spectrum of possible silk functions in Eriophyoidea (e.g., gluing the anal lobe to the substrate during overwintering and producing drag lines or assistance in the finding of conspecifics [18,19,43]) awaits experimental testing. If future studies confirm the presence of a silk-producing ASA in all members of Eriophyoidea, anal silk will become a new, unusual synapomorphy of this aberrant group of acariform mites.

The principal uniformity of the ASA suggests that its elements could be parsimoniously homologized, and the previously proposed terminology [18,73] could be applied as follows: the large glands are hypertrophied anal glands secreting silk; the dorsal and ventral sacs are derivatives of the rectal tube; the medial sac is the anterior section of the hindgut, (rectal sac); and the excretory channel leading to the anal opening is the rectal tube. The ventral and dorsal sacs apparently function as reservoirs for silk storage. Mites probably empty them via narrowing the caudal part of the opisthosoma or using their strong peripheral body muscles [18], causing internal hydraulic pressure.

Eriophyoid taxa differ in the degree of development of their midgut. Sparse published TEM observations suggest that in some taxa (a) the midgut is reduced and completely absent in the posterior half of the body [18,73,74], and storage of waste products happens in tissues [18]. In other taxa (b) the midgut is well-developed, with a large distal section (posterior midgut) that merges into the hindgut. In group (b), therefore, the intestine is continuous and can be used for feces excretion [73]. Contrary to our expectations, the results of this study suggest that *A. schotiae* n. sp. belongs to group (b) and possesses a median sac filled with amorphous matrix and joined anteriorly with putative posterior midgut. Therefore, the content of the median sac may be actual feces formed in the midgut. It is not clear if the contents of the midgut mix with silk and contribute to the web in *A. schotiae* n. sp. Due to suboptimal material fixation, we could not unambiguously reconstruct the tissue composition and reveal the visceral muscles of the ASA. If a muscular sphincter is present in the area where the rectal sac joins the rectal tube, the separation of silk and feces could be easily regulated. Comprehensive comparative TEM studies of different eriophyoid taxa are needed to reveal if the anatomies of the ASA and intestine in Eriophyoidea are correlated.

Taxonomical status and phylogenetic position of *Aberoptus* and *Cisaberoptus*. The presence of an ASA in phylogenetically distant eriophyoid taxa implies that, theoretically, strengthening the secretory activity of the ASA via hypertrophy of anal glands could homoplastically happen in non-related clades of Eriophyoidea. This thesis is in accord with our molecular phylogenetic results suggesting that web-spinning genera *Aberoptus* and *Cisaberoptus* belong to different eriophyoid lineages, dominated by morphologically dissimilar taxa (Figure 14).

This, however, does not exclude the possibility that *Cisaberoptus* has its own mechanism for silk production, e.g., based on hypertrophy of prosomal glands or “regurgitation” [32].

Although only two species of *Aberoptus* were included in our molecular phylogenetic analyses, they form a highly supported clade on the 28S tree, providing ample reasons to conclude that *Aberoptus* is monophyletic. This is to be expected, considering the negligible probability that unique leg morphology shared by all members of *Aberoptus* is homoplastic. Interestingly, a larger clade that comprises *Aberoptus* also includes members of *Aceria* and *Aculops* (Figure 14), the two genera morphologically corresponding to the non-spinning morphotype B of *Aberoptus*. This finding suggests that the highly specialized web-spinning genus *Aberoptus* could have originated from an *Aceria*-like ancestor. Note that the genus *Aceria* is a typical plesiomorphon [16], and no published study has inferred *Aceria* as monophyletic. Therefore, instead of synonymizing *Aberoptus* and *Aceria*, it is necessary to intensify phylogenetic studies of *Aceria* in order to find natural groupings within this enormously large [28] polyphyletic taxon and subdivide it into smaller monophyletic genera.

5. Conclusions

Recent discoveries of the ASA and identification of silk production as a function of anal glands gradually lead us to move from the paradigm of exoticism of web-spinning eriophyoid taxa [32] to the hypothesis of synapomorphic specialization of the hindgut to excrete the anal gland secretions in all Eriophyoidea. Silk production and modifications in the intestinal anatomy of gall mites are probably correlated phenomena that require further comparative histological studies.

The anal glands of all eriophyoids may be capable of synthesizing a silk-like secretion, which, along with other hypothetical functions, potentially facilitates the meeting of conspecifics [18] that is especially important for vagrant and un abundant species. If this hypothesis is correct, then the destruction of silk threads on the leaves (e.g., by spraying) or suppression of the silk genes, as was proposed for tetranychids [10], could help to control eriophyoid mites on crops and ornamental plants.

Due to their worm-like body and microscopic size, eriophyoid mites were considered tiny insect larvae when they were first noted inside leaf galls by zoologists about 300 years ago [24]. Our study shows that, along with a peculiar peripheral musculature [18] resembling that in dipteran larvae [75], eriophyoids have one more analogy that brings them closer to the larvae of some insects producing Malpighian tubule silks [2]—excretion of silk through the hindgut. This is a case of acquiring a novel vital function by the posterior body region leading to evolutionary success in extremely miniaturized arthropods, eriophyoid mites, and a unique example of anal silk secretion in Chelicerata.

Supplementary Materials: The following supporting information can be downloaded at: <https://www.mdpi.com/article/10.3390/d15020151/s1>, Figures S1–S8: additional LT-SEM images of *Aberoptus schotiae* n. sp.

Author Contributions: Conceptualization, P.E.C.; methodology, P.E.C., C.C. and A.E.V.; validation, C.C., V.D.G. and A.S.Z.; formal analysis, P.E.C., C.C. and A.E.V.; investigation, P.E.C., C.C. and A.E.V.; resources, data curation, V.D.G. and A.S.Z.; writing—original draft preparation, P.E.C., C.C. and V.D.G.; writing—review and editing, P.E.C. and C.C.; visualization, P.E.C., C.C. and A.E.V.; supervision, project administration, funding acquisition, P.E.C. All authors have read and agreed to the published version of the manuscript.

Funding: This research was funded by Ministry of Science and Higher Education of the Russian Federation (agreement 075-15-2022-322 “Agricultural technologies for the Future”).

Institutional Review Board Statement: Not applicable.

Data Availability Statement: The new sequences of *Aberoptus schotiae* n. sp. have been deposited in the National Center for Biotechnology Information (NCBI) GenBank database (<https://www.ncbi.nlm.nih.gov/genbank>) (accessed on 12 September 2022); accession numbers: OP419490 and OP419491.

Acknowledgments: We thank Evert E. Lindquist (Ottawa, Canada) for his remarks on the earlier version of the manuscript. We are grateful to Alan Urban (University of Pretoria, South Africa) for assisting with LTSEM and to Konstantin Benken (Saint-Petersburg State University, Russia) for his help with AFM. LTSEM was performed at the Laboratory for Microscopy and Microanalysis, University of Pretoria, South Africa. CLSM, AFM, TEM, LMSSS, PCR and sequencing were performed using equipment of The Centre for Molecular and Cell Technologies and The Centre for Microscopy and Microanalysis of The Research Park of Saint-Petersburg State University (Russia).

Conflicts of Interest: The authors declare no conflict of interest. The funders had no role in the design of the study; in the collection, analyses, or interpretation of data; in the writing of the manuscript; or in the decision to publish the results.

References

1. Craig, C.L. *Spiderwebs and Silk: Tracing Evolution from Molecules to Genes to Phenotypes*; Oxford University Press: New York, NY, USA, 2003; pp. 1–230.
2. Sutherland, T.D.; Young, J.H.; Weisman, S.; Hayashi, C.Y.; Merritt, D.J. Insect silk: One name, many materials. *Annu. Rev. Entomol.* **2010**, *55*, 171–188. [[CrossRef](#)] [[PubMed](#)]
3. Capinera, J.L. Silk. In *Encyclopedia of Entomology*; Capinera, J.L., Ed.; Springer: Dordrecht, The Netherlands, 2008; pp. 3373–3374. [[CrossRef](#)]
4. Schoeser, M. *Silk*; Yale University Press: New Haven, CT, USA, 2007; pp. 1–256.
5. Allmelting, C.; Jokuszies, A.; Reimers, K.; Kall, S.; Vogt, P.M. Use of spider silk fibres as an innovative material in a biocompatible artificial nerve conduit. *J. Cell Mol. Med.* **2006**, *10*, 770–777. [[CrossRef](#)]
6. Kluge, J.A.; Rabotyagova, O.; Leisk, G.G.; Kaplan, D.L. Spider silks and their applications. *Trends Biotechnol.* **2008**, *26*, 244–251. [[CrossRef](#)]
7. Lateef, A.; Ojo, S.A.; Elegbede, J.A. The emerging roles of arthropods and their metabolites in the green synthesis of metallic nanoparticles. *Nanotechnol. Rev.* **2016**, *5*, 601–622. [[CrossRef](#)]
8. Lozano-Pérez, A.A.; Pagán, A.; Zhurov, V.; Hudson, S.D.; Hutter, J.L.; Pruneri, V.; Pérez-Moreno, I.; Grbić, V.; Cenis, J.L.; Grbić, M.; et al. The silk of gorse spider mite *Tetranychus lintearius* represents a novel natural source of nanoparticles and biomaterials. *Sci. Rep.* **2020**, *10*, 1–14. [[CrossRef](#)] [[PubMed](#)]
9. Arakawa, K.; Mori, M.; Kono, N.; Suzuki, T.; Gotoh, T.; Shimano, S. Proteomic evidence for the silk fibroin genes of spider mites (Order Trombidiformes: Family Tetranychidae). *J. Proteom.* **2021**, *239*, 104195. [[CrossRef](#)] [[PubMed](#)]
10. Li, X.; Liu, R.; Li, G.; Jin, D.; Guo, J.; Ochoa, R.; Yi, T. Identification of the fibroin of *Stigmaeopsis nanjingensis* by a nanocarrier-based transdermal dsRNA delivery system. *Exp. Appl. Acarol.* **2022**, *87*, 31–47. [[CrossRef](#)]
11. Sombke, A.; Müller, C.H. When SEM becomes a deceptive tool of analysis: The unexpected discovery of epidermal glands with stalked ducts on the ultimate legs of geophilomorph centipedes. *Front. Zool.* **2021**, *18*, 1–19. [[CrossRef](#)]
12. Kovoov, J. Comparative structure and histochemistry of silk-producing organs in arachnids. In *Ecophysiology of Spiders*; Nentwig, W., Ed.; Springer: Berlin/Heidelberg, Germany, 1987; pp. 160–186. [[CrossRef](#)]
13. Hilbrant, M.; Damen, W.G. The embryonic origin of the ampullate silk glands of the spider *Cupiennius salei*. *Arthropod Struct. Dev.* **2015**, *44*, 280–288. [[CrossRef](#)]
14. Alberti, G.; Coons, L.B. Acari: Mites. In *Microscopic Anatomy of Invertebrates: Chelicerate Arthropoda*; Harrison, F.W., Foelix, R.F., Eds.; Wiley-Liss: New York, NY, USA, 1999; Volume 8, pp. 515–1265.
15. Shatrov, A.B.; Soldatenko, E.V. Organization of dermal glands and characteristic of secretion in the freshwater mite, *Limnesia maculata* (O. F. Müller, 1776) (Acariformes, Limnesiidae). *J. Morphol.* **2022**, *283*, 346–362. [[CrossRef](#)]
16. Kluge, N.J. *Insect Systematics and Principles of Cladoendesis*, 3rd ed.; KMK Scientific Press: Moscow, Russia, 2020; Volume 2, pp. 1–1037. (In Russian)
17. Weygoldt, P. Spermatophore web formation in a pseudoscorpion. *Science* **1966**, *153*, 1647–1649. [[CrossRef](#)]
18. Nuzzaci, G.; Alberti, G. Internal anatomy and physiology. In *Eriophyoid Mites: Their Biology, Natural Enemies and Control. World Crop Pests*; Lindquist, E.E., Sabelis, M.W., Bruin, J., Eds.; Elsevier Science Publishing: Amsterdam, The Netherlands, 1996; Volume 6, pp. 101–150. [[CrossRef](#)]
19. Chetverikov, P.E.; Bolton, S.J.; Gubin, A.I.; Letukhova, V.Y.; Vishnyakov, A.E.; Zukoff, S. The anal secretory apparatus of Eriophyoidea and description of *Phyllocoptes bilobospinosus* n. sp. (Acariformes: Eriophyidae) from Tamarix (Tamaricaceae) from Ukraine, Crimea and USA. *Syst. Appl. Acarol.* **2019**, *24*, 139–157. [[CrossRef](#)]
20. Norton, R.A.; Florian, M.L.E.; Manning, L.E. Ecdysial cleavage line in *Paralycus* sp. (Acari: Oribatida: Pediculochelidae). *Int. J. Acarol.* **2001**, *27*, 97–99. [[CrossRef](#)]
21. Shatrov, A.B.; Soldatenko, E.V.; Gavrilova, O.V. Observation on silk production and morphology of silk in water mites (Acariformes: Hydrachnidia). *Acarina* **2014**, *22*, 133–148.
22. Gerson, U. Webbing. In *Spider Mites: Their Biology, Natural Enemies, and Control*; Helle, W., Sabelis, M.W., Eds.; Elsevier Science Publishers: Amsterdam, The Netherlands, 1985; Volume 2, pp. 223–230.

23. Ray, H.A.; Hoy, M.A. Role of silk webbing in the biology of *Hemicheyletia wellsina* (Acari: Cheyletidae). *Int. J. Acarol.* **2014**, *40*, 577–581. [[CrossRef](#)]
24. Lindquist, E.E. External anatomy and notation of structures. In *Eriophyoid Mites: Their Biology, Natural Enemies and Control. World Crop Pests*; Lindquist, E.E., Sabelis, M.W., Bruin, J., Eds.; Elsevier Science Publishing: Amsterdam, The Netherlands, 1996; Volume 6, pp. 3–31. [[CrossRef](#)]
25. Bolton, S.J.; Chetverikov, P.E.; Klompen, H. Morphological support for a clade comprising two vermiform mite lineages: Eriophyoidea (Acariformes) and Nematolycidae (Acariformes). *Syst. Appl. Acarol.* **2017**, *22*, 1096–1131. [[CrossRef](#)]
26. Klimov, P.B.; OConnor, B.M.; Chetverikov, P.E.; Bolton, S.J.; Pepato, A.R.; Mortazavi, A.L.; Tolstikov, A.V.; Bauchan, G.R.; Ochoa, R. Comprehensive phylogeny of acariform mites (Acariformes) provides insights on the origin of the four-legged mites (Eriophyoidea), a long branch. *Mol. Phylogenet. Evol.* **2018**, *119*, 105–117. [[CrossRef](#)]
27. Klimov, P.B.; Chetverikov, P.E.; Dodueva, I.E.; Vishnyakov, A.E.; Bolton, S.J.; Paponova, S.S.; Lutova, L.A.; Tolstikov, A.V. Symbiotic bacteria of the gall-inducing mite *Fragariocoptes setiger* (Eriophyoidea) and phylogenomic resolution of the eriophyoid position among Acari. *Sci. Rep.* **2022**, *12*, 3811. [[CrossRef](#)]
28. Amrine, J.W., Jr.; Stasny, T.A.H.; Flechtmann, C.H.W. *Revised Keys to the World Genera of the Eriophyoidea (Acari: Prostigmata)*; Indira Publishing House: West Bloomfield, MI, USA, 2003; pp. 1–244.
29. de Lillo, E.; Pozzebon, A.; Valenzano, D.; Duso, C. An intimate relationship between eriophyoid mites and their host plants—A review. *Front. Plant Sci.* **2018**, *9*, 1–14. [[CrossRef](#)]
30. Neravathu, R. Feeding impact of *Cisaberoptus kenyae* Keifer (Acari: Eriophyidae) on photosynthetic efficiency and biochemical parameters of *Mangifera indica* L. *Acarol. Stud.* **2019**, *1*, 84–94.
31. Ivanova, L.A.; Chetverikov, P.E.; Ivanov, L.A.; Tumurjav, S.; Kuzmin, I.V.; Desnitskiy, A.G.; Tolstikov, A.V. The effect of gall mites (Acariformes, Eriophyoidea) on leaf morphology and pigment content of deciduous trees in West Siberia. *Acarina* **2022**, *30*, 89–98. [[CrossRef](#)]
32. Manson, D.C.M.; Gerson, U. Web spinning, wax secretion and liquid secretion by eriophyoid mites. In *Eriophyoid Mites: Their Biology, Natural Enemies and Control. World Crop Pests*; Lindquist, E.E., Sabelis, M.W., Bruin, J., Eds.; Elsevier Science Publishing: Amsterdam, The Netherlands, 1996; Volume 6, pp. 251–258. [[CrossRef](#)]
33. Britto, E.P.; Gondim, M.G., Jr.; Navia, D.; Flechtmann, C.H.W. A new deutergynous eriophyid mite (Acari: Eriophyidae) with dimorphic males from *Caesalpinia echinata* (Caesalpinaceae) from Brazil: Description and biological observations. *Int. J. Acarol.* **2008**, *34*, 307–316. [[CrossRef](#)]
34. Knorr, L.C.; Phatak, H.C.; Keifer, H.H. Web-spinning eriophyid mites. *J. Wash. Acad. Sci.* **1976**, *66*, 228–234.
35. Keifer, H.H. Eriophyid Studies XVII. *Bull. Calif. State Dept. Agric.* **1951**, *40*, 93–104.
36. Hassan, E.F.O.; Keifer, H.H. Mango leaf-coating mite, *Cisaberoptus kenyae* K. (Eriophyidae, Aberoptinae). *Pan. Pac. Entomol.* **1978**, *54*, 185–193.
37. Navia, D.; Flechtmann, C.H.W. Eriophyid mites (Acari: Prostigmata) from mango, *Mangifera indica* L., in Brazil. *Int. J. Acarol.* **2000**, *26*, 73–80. [[CrossRef](#)]
38. Flechtmann, C.H.W. *Aberoptus cerostructor* n. sp., a deutergynous species from Brazil (Acari: Eriophyidae). *Int. J. Acarol.* **2001**, *27*, 199–204. [[CrossRef](#)]
39. Smith Meyer, M.K.P. African Eriophyoidea: On species of the subfamily Aberoptinae (Acari: Eriophyidae). *Phytophylactica* **1989**, *21*, 271–274.
40. Elhalawany, A.S.; Amrine, J.W.; Ueckermann, E.A. A new species and new record of eriophyoid mites (Trombidiformes: Eriophyoidea) from mango in Egypt with a note on the population dynamics of four eriophyoid species. *Acarines* **2021**, *15*, 1–22. [[CrossRef](#)]
41. Chetverikov, P.E.; Desnitskaya, E.A.; Efimov, P.G.; Bolton, S.J.; Cvrković, T.; Petanović, R.U.; Zukoff, S.; Amrine, J.W., Jr.; Klimov, P. The description and molecular phylogenetic position of a new conifer-associated mite, *Setoptus tsugivagus* n. sp. (Eriophyoidea, Phytoptidae, Nalepellinae). *Syst. Appl. Acarol.* **2019**, *24*, 683–700. [[CrossRef](#)]
42. Chetverikov, P.E.; Craemer, C.; Cvrković, T.; Efimov, P.G.; Klimov, P.B.; Petanović, R.U.; Sukhareva, S.I. First pentasetacid mite from Australasian Araucariaceae: Morphological description and molecular phylogenetic position of *Pentasetacus novozelandicus* n. sp. (Eriophyoidea, Pentasetacidae) and remarks on anal lobes in eriophyoid mites. *Syst. Appl. Acarol.* **2019**, *24*, 1284–1309. [[CrossRef](#)]
43. Chetverikov, P.E.; Bertone, M. First rhyncaphyoptine mite (Eriophyoidea, Diptilomiopidae) parasitizing american hazelnut (*Corylus americana*): Molecular identification, confocal microscopy, and phylogenetic position. *Exp. Appl. Acarol.* **2022**, *88*, 75–95. [[CrossRef](#)] [[PubMed](#)]
44. Amrine, J.W., Jr.; Manson, D.C.M. Preparation, mounting and descriptive study of eriophyoid mites. In *Eriophyoid Mites: Their Biology, Natural Enemies and Control. World Crop Pests*; Lindquist, E.E., Sabelis, M.W., Bruin, J., Eds.; Elsevier Science Publishing: Amsterdam, The Netherlands, 1996; Volume 6, pp. 383–396. [[CrossRef](#)]
45. Chetverikov, P.E. Video projector: A digital replacement for camera lucida for drawing mites and other microscopic objects. *Syst. Appl. Acarol.* **2016**, *21*, 1278–1280. [[CrossRef](#)]
46. Echlin, P.; Paden, R.; Dronzek, B.; Wayte, R. Scanning electron microscopy of labile biological material maintained under controlled conditions. *Scan. Electron. Microsc.* **1970**, 49–56.

47. Kirejtshuk, A.G.; Chetverikov, P.E.; Azar, D. Libanopsinae, new subfamily of the family Sphindidae (Coleoptera, Cucujoidea) from Lower Cretaceous Lebanese amber, with remarks on using confocal microscopy for the study of amber inclusions. *Cretac. Res.* **2015**, *52*, 461–479. [[CrossRef](#)]
48. Chetverikov, P.E. Confocal laser scanning microscopy technique for the study of internal genitalia and external morphology of eriophyoid mites (Acari: Eriophyoidea). *Zootaxa* **2012**, *3453*, 56–68. [[CrossRef](#)]
49. Schneider, C.; Rasband, W.; Eliceiri, K. NIH Image to ImageJ: 25 years of image analysis. *Nat. Methods* **2012**, *9*, 671–675. [[CrossRef](#)]
50. Humphrey, C.D.; Pittman, F.E. A simple methylene blue-azure II-basic fuchsin stain for epoxy-embedded tissue sections. *Stain. Technol.* **1974**, *49*, 9–14. [[CrossRef](#)]
51. Katoh, K.; Misawa, K.; Kuma, K.; Miyata, T. MAFFT: A novel method for rapid multiple sequence alignment based on fast Fourier transformation. *Nucleic Acids Res.* **2002**, *30*, 3059–3066. [[CrossRef](#)]
52. Katoh, K.; Rozewicki, J.; Yamada, K.D. MAFFT online service: Multiple sequence alignment, interactive sequence choice and visualization. *Brief. Bioinform.* **2017**, *20*, 1160–1166. [[CrossRef](#)]
53. Minh, B.Q.; Schmidt, H.A.; Chernomor, O.; Schrempf, D.; Woodhams, M.D.; von Haeseler, A.; Lanfear, R. IQ-TREE 2: New Models and Efficient Methods for Phylogenetic Inference in the Genomic Era. *Mol. Biol. Evol.* **2020**, *37*, 1530–1534. [[CrossRef](#)] [[PubMed](#)]
54. Kalyaanamoorthy, S.; Minh, B.Q.; Wong, T.K.F.; von Haeseler, A.; Jermini, L.S. ModelFinder: Fast model selection for accurate phylogenetic estimates. *Nat. Methods* **2017**, *14*, 587–589. [[CrossRef](#)]
55. Chase, M.W.; Christenhusz, M.J.M.; Fay, M.F.; Byng, J.W.; Judd, W.S.; Soltis, D.E.; Mabberley, D.J.; Sennikov, A.N.; Soltis, P.S.; Stevens, P.F. An update of the Angiosperm Phylogeny Group classification for the orders and families of flowering plants: APG IV. *Bot. J. Linn. Soc.* **2016**, *181*, 1–20. [[CrossRef](#)]
56. Koenen, E.J.; Ojeda, D.I.; Steeves, R.; Migliore, J.; Bakker, F.T.; Wieringa, J.J.; Kidner, C.; Hardy, O.J.; Pennington, R.T.; Bruneau, A.; et al. Large-scale genomic sequence data resolve the deepest divergences in the legume phylogeny and support a near-simultaneous evolutionary origin of all six subfamilies. *New Phytol.* **2020**, *225*, 1355–1369. [[CrossRef](#)] [[PubMed](#)]
57. Chetverikov, P.E.; Craemer, C.; Nesor, S. New pseudotagmic genus of acaricaline mites (Eriophyidae, Acaricalini) from a South African palm *Hyphaene coriacea* and remarks on lateral opisthosomal spines and morphology of deutogynes in Eriophyoidea. *Syst. Appl. Acarol.* **2018**, *23*, 1073–1101. [[CrossRef](#)]
58. Krantz, G.W. Habit and habitats. In *A Manual of Acarology*, 3rd ed.; Krantz, G.W., Walter, D.E., Eds.; Texas Tech University Press: Lubbock, TX, USA, 2009; pp. 64–82.
59. Buzatto, B.A.; Machado, G. Male dimorphism and alternative reproductive tactics in harvestmen (Arachnida: Opiliones). *Behav. Process.* **2014**, *109*, 2–13. [[CrossRef](#)]
60. Cho, G.; Malenovský, I.; Burckhardt, D.; Inoue, H.; Lee, S. DNA barcoding of pear psyllids (Hemiptera: Psylloidea: Psyllidae), a tale of continued misidentifications. *B. Entomol. Res.* **2020**, *110*, 521–534. [[CrossRef](#)]
61. Manson, D.C.M.; Oldfield, G.N. Life forms, deutogyny, diapause and seasonal development. In *Eriophyoid Mites: Their Biology, Natural Enemies and Control. World Crop Pests*; Lindquist, E.E., Sabelis, M.W., Bruin, J., Eds.; Elsevier Science Publishing: Amsterdam, The Netherlands, 1996; Volume 6, pp. 173–183. [[CrossRef](#)]
62. Chetverikov, P.E.; Petanović, R.U. New observations on early-derivative mite *Pentasetacus araucariae* (Schliesske) (Acariformes: Eriophyoidea) infesting relict gymnosperm *Araucaria araucana*. *Syst. Appl. Acarol.* **2016**, *21*, 1157–1190. [[CrossRef](#)]
63. Chetverikov, P.E.; Rector, B.G.; Tonkel, K.; Dimitri, L.; Cheglakov, D.S.; Romanovich, A.E.; Amrine, J. Phylogenetic position of a new *Trisetacus* mite species (Nalepellidae) destroying seeds of North American junipers and new hypotheses on basal divergence of Eriophyoidea. *Insects* **2022**, *13*, 201. [[CrossRef](#)]
64. Keifer, H.H. Eriophyid Studies XII. *Bull. Calif. State Dept. Agric.* **1942**, *31*, 117–129.
65. Yin, Y.; Yao, L.F.; Zhang, Q.; Hebert, P.D.; Xue, X.F. Using multiple lines of evidence to delimit protogynes and deutogynes of four-legged mites: A case study on *Epitrimerus sabiniae* s.l. (Acari: Eriophyidae). *Invertebr. Syst.* **2020**, *34*, 757–768. [[CrossRef](#)]
66. Chetverikov, P.E.; Klimov, P.B.; He, Q. Vertical transmission and seasonal dimorphism of eriophyoid mites (Acariformes, Eriophyoidea) parasitic on the Norway maple: A case study. *Royal Soc. Open Sci.* **2022**, *9*, 220820. [[CrossRef](#)] [[PubMed](#)]
67. Chetverikov, P.E.; Craemer, C.; Bolton, S. Exoskeletal transformations in Eriophyoidea: New pseudotagmic taxon *Pseudotagmus africanus* ng & n. sp. from South Africa and remarks on pseudotagmosis in eriophyoid mites. *Syst. Appl. Acarol.* **2017**, *22*, 2093–2118. [[CrossRef](#)]
68. Doğan, S.; Çağlar, M.; Çağlar, B.; Çirak, Ç.; Zeytun, E. Structural characterization of the silk of two-spotted spider mite *Tetranychus urticae* Koch (Acari: Tetranychidae). *Syst. Appl. Acarol.* **2017**, *22*, 572–583. [[CrossRef](#)]
69. Guo, J.F.; Li, H.S.; Wang, B.; Xue, X.F.; Hong, X.Y. DNA barcoding reveals the protogyne and deutogyne of *Tegolophus celtis* sp. nov. (Acari: Eriophyidae). *Exp. Appl. Acarol.* **2015**, *67*, 393–410. [[CrossRef](#)]
70. Sabelis, M.W.; Bruin, J. 1996 Evolutionary ecology: Life history patterns, food plant choice and dispersal. In *Eriophyoid Mites: Their Biology, Natural Enemies and Control. World Crop Pests*; Lindquist, E.E., Sabelis, M.W., Bruin, J., Eds.; Elsevier Science Publishing: Amsterdam, The Netherlands, 1996; Volume 6, pp. 329–366.
71. Michalska, K.; Skoracka, A.; Navia, D.; Amrine, J.W. Behavioural studies on eriophyoid mites: An overview. *Exp. Appl. Acarol.* **2010**, *51*, 31–59. [[CrossRef](#)]
72. Navia, D.; Flechtman, C.H.W.; Lindquist, E.E.; Aguilar, H. A new species of *Abacarus* (Acari: Prostigmata: Eriophyidae) damaging sugarcane, *Sacharrum officinarum* L., from Costa Rica—The first eriophyoid mite described with a tibial seta on leg II. *Zootaxa* **2011**, *3025*, 51–58. [[CrossRef](#)]

73. Nuzzaci, G. Contributo alla conoscenza dell'anatomia degli acari eriofidi. *Entomologica* **1976**, *12*, 21–55. [[CrossRef](#)]
74. Silvere, A.P.; Stein-Margolina, V. *Tetrapodili. Microanatomy, Problems of Evolution and Interrelationship with Pathogens of Plant Diseases*; Valgus Press: Tallinn, Estonia, 1976; pp. 1–164.
75. Wipfler, B.; Schneeberg, K.; Löffler, A.; Hünefeld, F.; Meier, R.; Beutel, R.G. The skeletomuscular system of the larva of *Drosophila melanogaster* (Drosophilidae, Diptera)—A contribution to the morphology of a model organism. *Arthropod. Struct. Dev.* **2013**, *42*, 47–68. [[CrossRef](#)]

Disclaimer/Publisher's Note: The statements, opinions and data contained in all publications are solely those of the individual author(s) and contributor(s) and not of MDPI and/or the editor(s). MDPI and/or the editor(s) disclaim responsibility for any injury to people or property resulting from any ideas, methods, instructions or products referred to in the content.